Molecular and behavioral study of the *FoxP* locus in *Drosophila melanogaster*

DISSERTATION ZUR ERLANGUNG DES

DOKTORGRADES DER NATURWISSENSCHAFTEN (DR. RER. NAT.)

DER FAKULTÄT FÜR BIOLOGIE UND VORKLINISCHE MEDIZIN

DER UNIVERSITÄT REGENSBURG

vorgelegt von

Ottavia Palazzo

aus

Turin, Italien

im Jahr

2020

Das Promotionsgesuch wurde eingereicht am:
Datum – Date of application for admission

Die Arbeit wurde angeleitet von:
Prof. Dr. Björn Brembs

Unterschrift:
Ottavia Palazzo

Table of Contents

Abstract

The human *FOXP2* gene has been identified as a key component for the development of language. Such vocal learning is a form of motor learning that proceeds slowly from babbling in toddlers (or subsong in zebra finches) towards fluent speech in adults (or crystallized song in zebra finches). This particular learning process can be conceptualized as operant self-learning, in which the organism learns the correct actions only by evaluating the outcomes of its previous behavior, in the absence of other sensory cues. In the fruit fly *Drosophila*, the *dFoxP* orthologue has been shown to also be involved in operant self-learning of yaw torque (attempted rotations around the vertical body axis) in tethered flies, an experiment conceptually analogous to vocal learning. However, despite those findings, the expression, function and mechanisms of action of dFoxP remain to be elucidated. In this work, we thus generated four transgenic lines using the CRISPR/Cas9 technique to unravel the expression pattern of FoxP and its function in locomotor behavior and object fixation. We find that the different FoxP isoforms are expressed in neurons, but not in glia and that those isoforms are differentially expressed. Furthermore, we detect FoxP expression in, e.g., the protocerebral bridge, the fan shaped body and in motorneurons, but not in the mushroom bodies. Finally, we discover that FoxP expression during development, but not adulthood, is required for normal locomotion and landmark fixation in walking flies.

1. Introduction

1.1 Drosophila as a model organism

For over a century the fruit fly *Drosophila melanogaster* has been used as a powerful genetic tool for biological research (*Roote and Prokop 2013*) while helping founding the field of classical genetics. The reason why this insect has grown in importance in research during the decades are multiple: they are easy and cheap to keep, the generation time takes about 10 days, which allows a rapid research progression, furthermore they are particularly useful for performing both forward and reverse genetics (*Brembs 2016*). Moreover, what makes the fruit fly a perfect model organism for biologists is the rich availability of genetic tools developed in more than a century as well as well-organized databases and stock centers that allow to easily combine classic genetic approaches with molecular genetic ones. One of the molecular techniques that in the last decade have been utilized and optimized is the CRISPR/Cas9 system, which is significantly advancing the ability of researchers to engineer targeted genome modifications for functional studies of genes and genetic elements (*Gratz et al., 2015*). Ultimately, another reason for the fly's success in biological research is their ease of handling, that together with their ability to perform many behaviors (from simple motor actions to complex social interactions), makes them particularly suitable to be used for various behavioral paradigms (*Sokolowski, 2001*).

1.2 CRISPR/Cas9 as a powerful genetic tool in flies

As previously said, one of the molecular techniques that have known drastic advancement in the last decade is the DNA modification by CRISPR/Cas9 (Clustered Regularly Interspaced Short Palindromic Repeats/Cas9). In 2012, Doudna and Charpentier were the first to propose that CRISPR/Cas9 could be used for programmable editing of genomes (*Jinek et al., 2012*).

This mechanism is born in bacteria and archaea as a defense system developed to resist viral infections (*Horvath and Barrangou, 2010*). The main components of this immune response are firstly the short palindromic repeats, which are interspaced by spacer DNA regions that are identical to ones of bacteriophages, while the second components are

the *Cas* genes, which will generate the Cas proteins that are going to act as helicases and endonucleases. When the attacking bacteriophage injects the DNA in the receiving bacterial cell, the latter will transcribe the Cas proteins and the spacer DNA (that recognize the injected sequence), which together are going to neutralize the foreign piece of DNA.

This system can then be engineered and optimized in order to be used in all living cells to modify pieces of chosen genome in a precise fashion. This can be achieved by simply using the single Cas protein from *Streptococcus pyogenes* (the Cas9) *(Jinek et al., 2012)* and an engineered gRNA (that roughly corresponds to the RNA transcribed from the spacer DNA in bacteria) which is assembled in order to contain a sequence homologous to the one in the correct place in the target genome.

The first approach of this technology that was used to mutate the DNA of living cells is based on the non-homologous end joining mechanism (NHEJ) (*Lieber, 2010*), which exploits the natural repair mechanism that is most active in the cells. At its core, in NHEJ the broken ends can be ligated without a homologous template and it is susceptible to frequent mutation errors due to nucleotide insertions and/or deletions (indels). The second approach that could be used is instead the homologous directed repair (HDR) (*Heyer et al., 2010*; *Gratz et al., 2014*). In this case the repair of the broken DNA strands will occur in a more precise fashion thanks to the presence of a homologous template. It is important to mention that in most cells, both of these repair pathways are active, however the HDR pathway is generally less efficient that the NHEJ pathway in the absence of a homologous template (*Iliakis et al., 2004*).

1.2.1 HDR in flies

The previously mentioned HDR technique, being the more versatile and precise one, has now been widely used and optimized for the fruit fly. The strong point of this system is that it employs homologous DNA sequences as templates for precise repair, allowing the precise incorporation of exogenous DNA fragments (e.g. Gal4, the driver component from the UAS/Gal4 system, *Duffy, 2002*), including visual markers to aid during the screening (*Gratz et al., 2014*). It roughly consists in the creation of a vector incorporating the two homology inserts and the screenable marker (e.g. the fluorescent 3xP3-DsRed (*Horn and Handler, 2005*)), (Fig. 1.1) flanked by LoxP sites, plus the creation

of the vector(s) containing the sequence for the gRNA(s). The constructs will be subsequently injected into fly embryos which express Cas9 in the germline under the regulatory control of *vasa* (*Kondo and Ueda, 2013; Bassett and Liu, 2014*). Ultimately, this cassette could be easily accessed at a later time thanks to the presence of the LoxP sites in order to eliminate the visible marker (CRE-mediated removal).

To sum up, this technique can be used to precisely modify DNA by the insertion of exogenous sequences in the gene of interest thanks to homologous repair. It is important to mention that the results will change depending on using one or two gRNA: using one single gRNA will result in the clean insertion of DNA, while using two gRNA, besides the insertion of the DNA (e.g. the visible marker), will result in the deletion of part of the gene sequence.

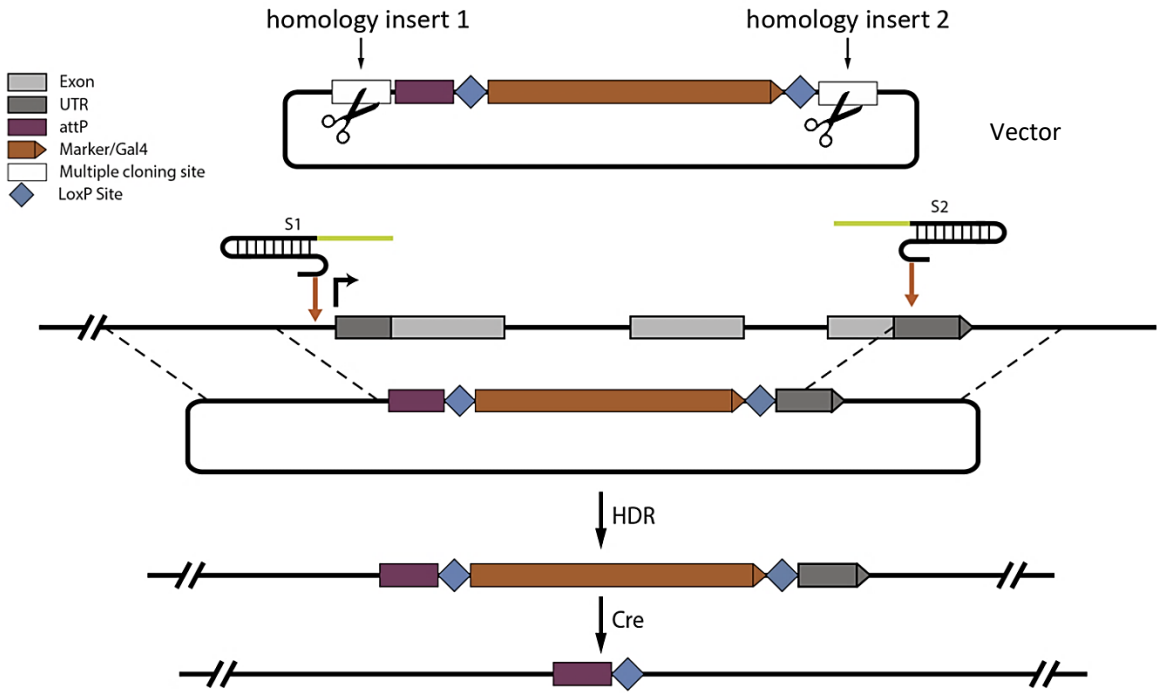

Fig. 1.1: *CRISPR/Cas9 HDR*. Graphic explanation of an example of the CRISPR/Cas9 HDR technique. Here we firstly see the vector with the two homology domains, subsequently, we see the gRNAs (S1 and S2) that will guide the Cas9 in the correct place in the genome where the cut will be performed. Thanks to the presence of the homologous template (the homology inserts in the vector) the repair of the broken DNA will be specific and DNA fragments will be exchanged. It will be possible to access the cassette again later and remove the visible marker, if required, thanks to a CRE-mediated cut in the LoxP sites. Modified from *Gratz et al., 2014*.

1.2.2 tRNA-based vectors

Another CRISPR/Cas9 technique that has been particularly useful to modify target DNAs is based on the production of multiple gRNAs starting from a single construct (*Xie et al., 2015*; *Port and Bullock, 2016*). In this technique are used plasmids (vectors) that are inspired by a tRNA-gRNA expression system in which the endogenous tRNA processing machinery liberates multiple functional gRNAs from a single precursor transcript in the nucleus. Once the gRNAs are processed and freed from the neighboring tRNAs, they will recognize the right sequences in the host genome and, in the presence of a Cas9, the cut will be performed. Where there are multiple gRNAs, multiple cuts will occur, likely producing frameshifts, and the gene will be mutated.

When the cloned plasmid is injected in a recombinant fly embryo containing an integrase and attP sites, it will integrate in the genome thanks to the attB sites found in the plasmid itself. Ultimately, it is important to mention that if tRNA-gRNA sequences are under the expression of a UAS promoter (the effector component from the UAS/Gal4 system), what it is obtained is a conditional line, where the KO can be induced at a chosen time or place, just by the election of the appropriate driver line.

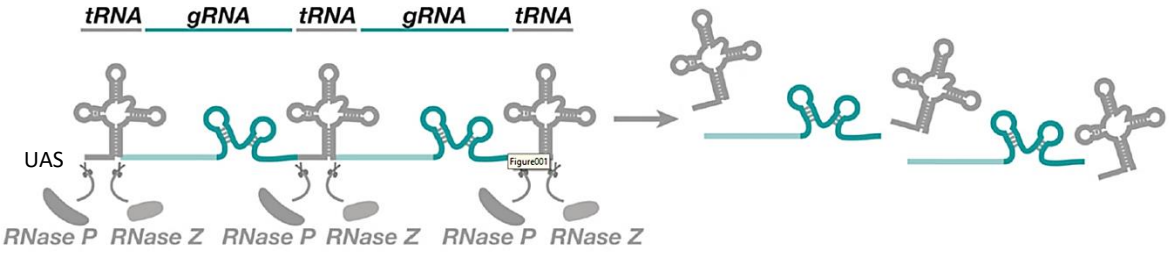

Fig. 1.2: *CRISPR/Cas9 tRNA-based vectors technique.* Schematic representation of part of the vector used for the CRISPR/Cas9 tRNA-based vectors technique: a chosen number of tRNAs and gRNAs sequence are found behind a UAS promoter. The tRNA processing machinery (RNases) liberates multiple functional gRNAs from a single precursor transcript, which are going to collaborate with the Cas9 in order to mutate the genome. Modified from *Port and Bullock 2016*.

1.3 The Fox genes

The family of *Fox* genes groups a large number of transcription factors that share a common sequence-specific DNA binding domain: the forkhead domain. It is an evolutionary ancient family of genes and the first member was discovered in *Drosophila*

(*Weigel et al., 1989*), in which, when mutated, gives the insect the typical fork-head appearance.

In eukaryotes, the forkhead domain has been identified in organisms starting from unicellular to fungi and finally animals, but not in plants (*Hannenhalli and Kaestner 2009; Shimeld et al., 2009*). There are 50 FOX genes in the human genome, around 44 in the mouse genome and 18 in *Drosophila*, which, up till now, have been classified and divided in 19 subfamilies (from FoxA to FoxS). It has been shown that they serve a wide range of functions, spanning from the regulation of glucose homeostasis (FoxO), to chromatin remodeling (FoxA) and vocal learning (FoxP) (*Jackson et al., 2010*). This latter subfamily of the Fox genes has grown in relevance in the last 20 years because of its important role for speech acquisition in humans.

1.3.1 FoxP in vertebrates

The FoxP subfamily has a distinguishing feature: besides the forkhead domain, it possesses another conserved domain called leucine zipper, which allows the components of the subfamily to form homodimers and heterodimers. The possibility to form heterodimers is due to the fact that in vertebrates there are 4 FoxP paralogues: FoxP1-4 (*Takahashi et al., 2009*; *Song et al., 2012; Bacon and Rappold, 2012*). The presence of 4 members is likely due to the occurrence of three duplication events after the evolutional split of vertebrates from invertebrates (*Santos et al., 2011*) (Fig. 1.3). Each of the different paralogues is expressed in different tissues and serves different functions, coordinating important developmental processes within various organs (*Golson and Kaestner, 2016*): FoxP1 regulates the development of lungs, heart, brain and gut (*Wang et al., 2004*; *Shu et al., 2007; Horn et al., 2010*), FoxP2 is widely expressed in the nervous tissue and, in humans and birds, is associated to vocal learning (*Chabout et al., 2016; Schatton and Scharf, 2016; Reuter et al., 2017; French et al., 2019; Co et al., 2020*), FoxP3 regulates T-cell specification and is important in the immune system (*Fontenot et al., 2003*), while FoxP4 is expressed during the development of lungs and gut (*Lu et al., 2002*).

FoxP1 and FoxP2 in particular, have been studied extensively in birds and mammals (especially humans) because of their linkage to neurodevelopmental disorder,

including autism spectrum disorder (ASD), intellectual disability (ID) and speech and language disorders.

Deletions or mutations (the vast majority of them in the DNA binding domain) of the FoxP1 paralogue in humans lead to a neurodevelopmental disorder named FOXP1 syndrome (*Siper at al., 2017*). People affected by this disease present a broad spectrum of symptoms like language impairment, ASD, ID and complex psychiatric presentations characterized by anxiety, obsessive-compulsive traits, and attention deficits (*Horn et al., 2010*; *Palumbo et al., 2013*; *Siper at al., 2017; Meerschaut et al., 2017*).

Mutations of FoxP2 lead instead to more selective deficits if compared to the ones caused by its close paralog FoxP1, most of them in the sphere of language acquisition. It was the first gene discovered to be involved in this kind of disability after the recognition of an autosomal point mutation in a multigenerational family ("KE" family) exactly in the fork head domain, which impairs the ability of the protein to bind DNA *(Lai et al., 2001*). The people affected by this monogenic disease present apraxia of speech and orofacial dyspraxia, and the areas of the brain that seems to be affected by FOXP2 mutations are cortex, cerebellum and the basal ganglia (*Chabout et al., 2016; Schatton and Scharff, 2016*; *Reuter et al., 2017; French et al., 2019; Co et al., 2020*).

Due to the human relevance, FoxP2 has been greatly studied in numerous model organisms, for example in mice, where it was analyzed in the cortex, striatum and cerebellum (*den Hoed and Fisher, 2020*). However, even though mice are more closely related to human, the greatest efforts for the study of FoxP2 have been done in birds (zebra finches), because of the parallelisms between the circuitries encoding birdsong and human speech (*Doupe and Kuhl, 1999*). In this species of birds, similar to human imitative learning, the song is learned by mimicking of conspecific, and young males learn the songs from an adult male tutor. This behavior relies on a set of brain nuclei collectively known as the song control circuit (*Heston and White, 2015*). The neural expression patterns of FoxP2 are conserved between humans and songbirds (*Enard, 2011; Heston and White, 2015*), including expression in the basal ganglia. In zebra finches in particular, FoxP2 is enriched in Area X, which is the song-dedicated basal ganglia nucleus necessary for vocal learning (*Haesler et al., 2004; Haesler et al., 2007*). The knockdown of FoxP2 in Area X of juvenile

males leads to inaccurate song learning, indicating that adequate FoxP2 levels are necessary for normal vocal learning (*Haesler et al., 2004; Haesler et al., 2007*; *Kosubek-Langer and Scharff 2020*).

This kind of vocal learning, that proceeds slowly from babbling in toddlers (or subsong in zebra finches) towards fluent speech in adults (or crystallized song in zebra finches), is a kind of motor learning that can be conceptualized as operant self-learning (counterposed to operant world-learning), in which the organism learns the correct actions to perform only by evaluating the outcomes of its previous behavior, in the absence of other sensory cues (*Skinner, 1938; Skinner, 1963; Brembs, 1996; Brembs and Heisenberg, 2000; Brembs and Heisenberg, 2001*).

1.3.2 FoxP in Drosophila

As previously stated, the original *forkhead* (*fkh*) gene was identified in the fruit fly *Drosophila melanogaster* (*Weigel et al., 1989*), where mutations cause defects in head fold involution during embryogenesis, causing the characteristic "fork head". In contrast to chordates with four FoxP family members, only one orthologue of the FoxP subfamily is present in flies (*dFoxP*), which originates three different transcripts by alternative splicing (*Castells-Nobau et al., 2019; Mendoza et al., 2014; Santos et al., 2011*): FoxP-isoform A (FoxP-iA), FoxP-isoform B (FoxP-iB) and FoxP-isoform IR (Intron Retention; FoxP-iIR) (Fig. 3.1A). Comparison of the protein sequences of the forkhead domain of dFoxP and murine FoxP1-4 orthologues reveal a high degree of conservation, with an overall of 62 % amino acids identity (*Santos et al., 2011*). The only paralogue in mice that conserve the alternative splicing is FoxP1 which, therefore, is the most closely related to the invertebrate FoxP, at least at the gene structure level (Fig. 1.3).

Analogous to vocal learning, data suggest that FoxP in *Drosophila* is involved in the same kind of learning of another orthologue: FoxP2. Operant self-learning of yaw torque (attempted rotations around the vertical body axis) in tethered flies is conceptually analogous to vocal learning: flies tethered at a torque meter first initiate variable exploratory actions followed by a reduction in behavioral variability as a result of sensory feedback (*Guo et al., 1996*; *Ernst and Heisenberg, 1999; Brembs and Heisenberg, 2000; Brembs and Heisenberg, 2001; Brembs and Wiener, 2006*). Thus, also in flies, alterations

of the dFoxP gene cause deficits in operant self-learning. Furthermore, data suggest that FoxP-iB, in particular, may be specifically important for operant self-learning *(Mendoza et al., 2014*).

However, besides the studies performed on operant self-learning, there are still contradicting evidences on where *dFoxP* is expressed and in which circuitries it participates *(DasGupta et al., 2014; Lawton et al., 2014; Groschner et al., 2018; Castells-Nobau et al., 2019*).

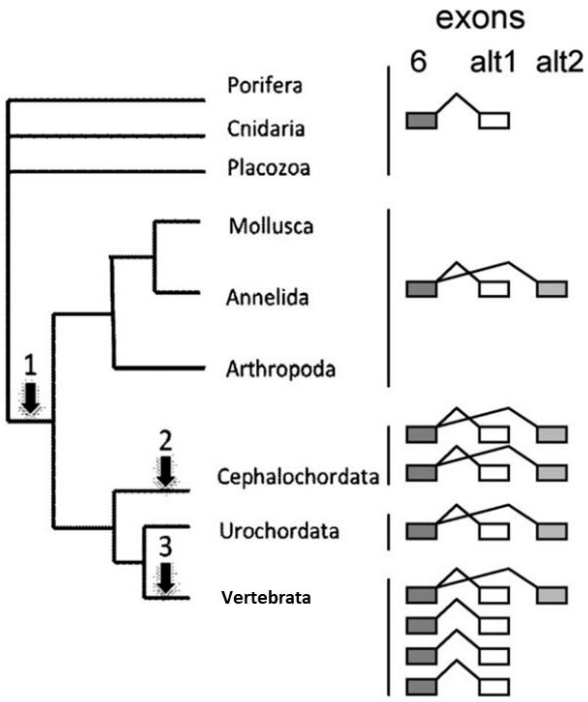

Fig. 1.3: *Main events of FoxP gene structure evolution in the animal reign.* In the diagram on the left he three arrows shows the duplication events. In the diagram on the right are shown the form of alternative splicing. Only the 6th and the 7th – 8th exons are shown. Modified from *Santos et al., 2011*.

1.4 Aim of the study

The currently available reports as to the expression pattern of the *FoxP* gene have been contradictory (*DasGupta et al., 2014; Lawton et al., 2014; Groschner et al., 2018; Castells-Nobau et al., 2019*) and nothing is known as to whether the different isoforms are differentially expressed in different cell types, as well as the role that they play in each of the nervous system areas. Furthermore, the tools that have been developed so far to study this gene have demonstrated to be obsolete and contradicting, thus leading to potential misconceptions.

In order to shed some light on this gene, in this work we exploit state of the art CRISPR/Cas9 techniques to specifically target the different isoforms of dFoxP directly in the gene locus, firstly to see their expression pattern, and subsequently to understand their involvement in motor behavior. We find out that different isoforms of dFoxP are differentially expressed in various cell types and neuropils of the fly brain (and ventral nerve cord), but not in the mushroom bodies, and, furthermore, we demonstrate that dFoxP is required for normal locomotion and object fixation, especially during development.

2. Materials and methods

2.1 Fly strains

Fly stocks were reared on standard food (Agar 0.8 %, sugar molasses 2.2 %, malt extract 8 %, yeast 1.8 %, soy flour 1 %, corn flour 8 %, Nipagin 0.3 %) and maintained at 18 °C (Table 1). Before experimental use, flies were kept at 25 °C, in a 12/12 hours light/dark regime at 60 % relative humidity for at least one generation. All crosses were raised at 25 °C (except for the ones involving the temperature sensitive Gal4 inhibitor Tub-Gal80ts (*McGuire et al., 2003; 2004*) that were raised at 18 °C) using 4-6 females and 2-4 males. For expression pattern visualizations, the *FoxP-iB-Gal4* and *FoxP-LexA* driver line, respectively, were crossed with the appropriate effector lines containing different GFP or RFP variants (Table 2.1). For behavioral analysis involving the *UAS-t:gRNA(4xFoxP)* effector line we crossed it first with *UAS-Cas9*, and subsequently with the appropriate driver line for each experiment (*ELAV-Gal4, D42-Gal4, C380-Gal4, cmpy-Gal4, ato-Gal* and *ELAV-Gal4;Tub-Gal80ts*). For conditional knock-out experiments, two genetic constructs need to be brought together for the method to work. The endonuclease Cas9 needs to be present as well as the guide RNA to provide a target for the nuclease. Hence, the appropriate control groups express only one component of the CRISPR/Cas9 combination. One line drives expression only of the Cas9 endonuclease (i.e., *xxx-Gal4>UAS-Cas9,* without gRNAs) and the other drives expression only of the gRNAs (i.e., *xxx-Gal4>UAS-t:gRNA(4xFoxP)* without Cas9). In this fashion, each strain not only controls for potential insertion effects of the transgenes used, but also for potential detrimental effects of expressing the components alone, irrespective of the excision of the target gene. For the behavioral analysis involving the *FoxP-KO* mutant and the *FoxP-iB-Gal4* driver line we performed a backcrossing with a *WTB* strain in order to get the same genetic background as the *WTB* control.

2.2 In-silico sequences alignment

The transcript and protein sequences of the different *FoxP* isoforms were downloaded from https://flybase.org and aligned with *Clustal Omega* for multiple sequence

alignment. The protein domains were analyzed with the *NCBI Conserved Domain Search* tool, and the stop codons were identified with *ExPASy Translate* tool (Fig. 3.1A).

2.3 Transgenic flies generation

We used CRISPR/Cas9 Homology Directed Repair (HDR) to edit the *FoxP* locus (*Gratz et al., 2014*) and generated t-RNA based vectors for producing multiple clustered regularly-interspaced (CRISPR) gRNAs from a single transcript (Port et al., 2016). We created a total of two driver lines (*FoxP-iB-Gal4* and *FoxP-LexA*), one mutant line (*FoxP-KO*) and one effector line (*UAS-t:gRNA(4xFoxP)*). For the first 3 fly lines, that were created with the HDR technique (*Gratz et al., 2014*), we followed a protocol of PCR-amplification (Table 2.2) of the homology insert from genomic DNA of *Vas/Cas9* flies (10 µl Phusion buffer (Table 2.3), 0.5 µl Phusion polymerase, 1 µl dNTPs, 2.5 µl fw primer, 2.5 µl rv primer, 1 µl template DNA, to 50 µl sterile H_2O), the amplicons were run on Agarose (0.8 %) gel to have a size dependent electrophoretic separation where the electrophoresis was performed at 120 V. Subsequent extraction of the bands from Agarose gel was performed following the E.Z.N.A. Gel Extraction Kit from VWR/Omega (Table 2.3), restriction enzyme digestion of both the inserts and the vector (5 µl Cutsmart buffer, 1 µl restriction enz.1, 1 µl restriction enz.2, all from New England BioLabs (Table 2.3), 5 µl vector or 25 µl insert, to 50 µl sterile H_2O) was then performed and left overnight in a water bath at 37 °C. Next, after the restriction reaction, we again performed the gel extraction procedure. The subsequent ligation reaction was carried out for 1 night at 18 °C, with a vector amount of 50 ng and with a vector to insert ratio of 1 to 3 that is usually used for cohesive end ligations (50 ng vector, X ng insert, 1 µl T4 Ligation buffer and 1 µl T4 DNA ligase from Thermo Fisher Scientific (Table 2.3), to 10 µl sterile H_2O). Subsequently, we performed the heatshock transformation using competent *DH5α-E. coli* which were finally plated on a petri dish and put overnight at 37 °C. As a control we performed the same ligation procedure and heatshock transformation with the same vector which however had no insert to incorporate. The subsequent day a colony PCR (Table 2.4) was performed in order to find clones which had incorporated the ligated plasmid: 20 single colonies were

chosen randomly from the petri dish with sterile pipette tip and each one was rinsed in its PCR reaction cup and then put into a test tube with 3 ml of LB amp selection medium (2 µl LSB buffer, 1 µl Taq polymerase (Table 2.3), 1 µl dNTPs, 1 µl fw primer, 1 µl rv primer, to 20 µl sterile H_2O). The clones that resulted positive in the PCR were let grow on a shaker overnight at 37 °C and then midiprepped following the Qiafilter Midi-Kit from QIAGEN protocol (Table 2.3). This procedure was then performed a second time in order to incorporate the second homology insert into the vector. Finally, we created the vector containing the gRNAs following a similar procedure: digestion of the appropriate vector (15 µl vector, 2 µl NEB 2.1 buffer and 1 µl restriction enz. from New England BioLabs (Table 2.3), to 20 µl sterile H_2O) and annealing of the oligos (1 µl oligo 1, 1 µl oligo 2, 1 µl T4 Ligase buffer, 1 µl T4 polynucleotide kinase from New England BioLabs (Table 2.3), to 10 µl H_2O), gel extraction, ligation, heatshock transformation, colony PCR and midiprep as previously explained. All constructs were verified via the Sanger sequencing LightRun Tube of Eurofins Genomics: the DNA was diluted to a suitable concentration in 7.5 µl and 2.5 µl of M13 primer (fw or rv) were added (10 µM). Here follow the specifics for each different line that we cloned:

FoxP-iB-Gal4: To create an isoform-specific driver line, we inserted a *Gal4* sequence into exon 8, which is specific to isoform B. Two 1 kb homology fragments were PCR-amplified (primers Hom1: fw 5'-GGGGGCGGCCGCCGTGGAAGGTAAAATGCCCCATATATG-3', rv 5'-GGGGCCGCGGCCCTCGTGTAAGGAAAGGTTCGTACGAATCGC-3'; primers Hom2: fw 5'-GGGGGGCGCGCCACAAGTGCTTTGTACGTTATGAA-3', rv 5'-GGGGGGTACCGGTCACTGAGTATCGTTAATGATC-3') and digested with the appropriate restriction enzymes (Hom1: NotI and SacII, Hom2: AscI and KpnI) to be ligated in the pT-GEM(0) (Addgene plasmid # 62891; RRID: Addgene_62891) vector (*Diao et al., 2015*) which contained a Gal4 sequence and a 3xP3-DsRed-SV40 sequence for selection of transformants. The gRNA sequences used are: sense 5'-CTTCGACGTACAAAGCACTTGTGTA-3', and asense 5'-AAACTACACAAGTGCTTTGTACGTC-3'. They were annealed and cloned inside a pU6-gRNA (Addgene plasmid # 53062; RRID:Addgene_53062) vector (*Shan et al., 2013*), previously digested with BbsI restriction enzyme.

FoxP-LexA: To create a driver line that reflects expression of all FoxP isoforms, we inserted a *LexA* sequence into exon 3. Two 1 kb homology fragments were PCR-amplified (primers Hom1: fw 5'-GGGGGCGGCCGCCAGGAATGGCGGCATATGAGT-3', rv 5'-GGGGCCGCGGCCCTCTATTACGGTAAGCGGACTCCGG-3'; primers Hom2: fw 5'-GGCCGGTACCATAGCATAGGCCGACCCATC-3', rv 5'-GGCCACTAGTTCACATTCTCAACCCGCATAAAGC-3') and digested with the appropriate restriction enzymes (Hom1: NotI and SacII, Hom2: KpnI and SpeI) to be ligated in the pT-GEM(0) vector which contained a LexA sequence and a 3xP3-DsRed-SV40 sequence for selection of transformants. The gRNA sequences used are: sense 5'-CTTCGGGTCGGCCTATGCTATTTA-3', asense 5'-AAACTAAATAGCATAGGCCGACCC-3'. They were annealed and cloned inside a pU6-gRNA vector previously digested with BbsI restriction enzyme.

FoxP-KO: To prevent expression of any isoform of the FoxP gene, we removed part of exon 1, the complete exon 2 and part of exon 3. Two 1 kb homology fragments were PCR-amplified (primers Hom1: fw 5'-GGGGCTAGCCAAAATAAGATGTGTCTGGTTTCCTTG-3', rv 5'-GGGCCGCGGGCATGGCGAACTCATCGTG-3', primers Hom2: fw 5'-GGGGACTAGTAGAGGGAAAGTTTTGCCGG-3', rv 5'-GGGGCTGCAGTATGAAGGGACAGATTGTGCCGG-3') and digested with the appropriate restriction enzymes (Hom1: NheI and SacII, Hom2: SpeI and PstI) to be ligated in the pHD-DsRed-attP (Addgene plasmid # 51019; RRID: Addgene_51019) vector which contains a 3xP3-DsRed sequence for selection of transformants. The gRNA sequences used are: gRNA1 sense 5'-CTTCGCGGATGATAGTACTTCCGCA-3', asense 5'-AAACTGCGGAAGTACTATCATCCGC-3'; gRNA2 sense 5'-CTTCGAAGGACGTGCCCGGAAGAGA-3', asense 5'-AAACTCTCTTCCGGGCACGTCCTTC-3'. They were annealed and were cloned inside a pU6-gRNA vector previously digested with BbsI restriction enzyme.

For the creation of the last fly line, we followed a different cloning strategy based on *Port et al., 2016*. Selected oligos which allowed cloning 4 gRNAs from 3 overlapping PCR products, were PCR amplified (Table 2.2) with the vector backbone as a template (previously digested with the appropriate restriction enzyme as previously described) (10 μl

Q5 polymarease buffer, 0.5 µl Q5 polymerase (Table 2.3), 1 µl dNTPs, 2.5 µl fw primer, 2.5 µl rv primer, 1 ng vector DNA, to 50 µl sterile H_2O). Subsequently, an electrophoresis run and a gel extraction protocol, as previously described, were performed. Next, we performed a Gibson Assembly reaction (50 ng of digested plasmid, 2 fold molar excess of each insert, 10 µl NEBuilder HiFi DNA Assembly Master Mix from New England BioLabs (Table 2.3), to 20 µl sterile H_2O) which consists in the cloning of the oligos in a linearized plasmid (restriction enzyme digestion as previously explained) for 60 minutes at 50 °C. The following steps of the cloning are equivalent the ones explained previously. Here follow the specifics for this cloning procedure:

UAS-t:gRNA(4xFoxP): To create a UAS isoform-unspecific conditional effector line we phosphorylated and annealed 3 sets of oligos (1. fw 5'-CGGCCCGGGTTCGATTCCCGGCCGATGCAGAGCATCGATGAATCCTCAAGTTTCAGAGCTATGCTGGAAAC-3', rv 5'-GCTCGGATATGAACTCGGGCTGCACCAGCCGGGAATCGAACC-3'; 2. fw 5'-GCCCGAGTTCATATCCGAGCGTTTCAGAGCTATGCTGGAAAC-3', rv 5'-ACGGCATATGCCATGAGCAATGCACCAGCCGGGAATCGAACC-3'; 3. fw 5'-TTGCTCATGGCATATGCCGTGTTTCAGAGCTATGCTGGAAAC-3', rv 5'-ATTTTAACTTGCTATTTCTAGCTCTAAAACAACCATGTTCCGTATTCAGATGCACCAGCCGGGAATCGAACC-3') that were cloned with a single Gibson Assembly reaction in a pCFD6 (Addgene plasmid # 73915; RRID: Addgene_73915) vector (*Port and Bullock, 2016*) which was previously digested with BbsI restriction enzyme.

After the constructs were created, they were eluted in Ampuwa® water, diluted to the needed concentration and supplemented with a suitable amount of Injection Buffer (10x; KCl 5 mM, NaPO4 (pH 6.8) 0.1 mM) to be injected into dechorionated early embryos (30-45 min old) (;*Vas-Cas9;* for the *FoxP-iB-Gal4, FoxP-LexA* and *FoxP-KO* and *Integrase(x);;AttP2* for *UAS-t:gRNA(4xFoxP)).* The resulting transformants were selected and crossed two times with the balanced flies *w-;;D3/TM3, Sb*.

2.4 Immunohistochemistry

Three to six days-old adults were fixated in 4 % paraformaldehyde (PFA) at 4 °C for 2 hrs (30 minutes for the staining involving the FoxP antibody) and dissected in phosphate-buffered saline with 0.01 % Triton X-100® detergent (PBST). For larval staining, 3rd instar larvae were selected, dissected in 0.01 % PBST and fixated in 4 % PFA at room temperature (RT) for 30 min. Clean brains were washed 3 times in 0.01 % PBST for a total time of 45 min and then blocked with 10 % normal goat serum (NGS) for 1 hr. Subsequently, the brains were incubated with the appropriate primary antibody for 1-2 nights at 4 °C (Table 2.5). After 3 washing steps of 15 min each, the brains were incubated with the secondary antibody (Table 2.6) for 5-7 hrs at RT. After an additional 15 min washing step, the brains were placed on glass microscope slides and mounted with the antifade mounting medium Vectashield (Vector Laboratories, Burlingame, CA).

2.5 Image acquisition and analysis

All of the images were acquired with a Leica SP8 confocal microscope (RRID: SCR_018169), images were scanned at a frame size of 1024x1024 pixels at 200 or 100 Hz. The objectives were 20x dry and 20x/40x/60x oil immersion. Images were processed with ImageJ software (National Institutes of Health, USA) (RRID: SCR_003070) (*Rueden et al., 2017*), only general adjustments to color, contrast, and brightness were made. The cell counting was performed with IMARIS 9.0 (Oxford instruments) software on *UAS-Stinger-GFP* stacks, using the *Spots* tool for spots counting. For the *FoxP-iB-Gal4/FoxP-LexA* count (Fig. 3.5B), five brains were counted for each genotype at both larval (3rd instar) and adult (3 days old) stages. The colocalization analysis was performed with the ImageJ *Colocalization Threshold* tool (*Tony Collins* and *Daniel James White*) (Fig 3.6B).

2.6 RT-qPCR

The knockout efficiency was assessed using RT-qPCR (see Figs. 3.1D, 3.5E). We extracted RNA from 20 flies for each genotype (*white* ¯, heterozygous mutant and homozygous mutant, both backcrossed to *white* ¯) (Table 2.1), following a protocol from peqGOLD TriFast of VWR (Table 2.3). The RNA was subsequently transcribed into cDNA

following the OneStep RT-PCR Kit from QIAGEN (Table 2.3) (1 µl gDNA wipe out buffer 7x, 500 ng of template RNA, to 7 µl H_2O; followed by the addition, after the pause of the PCR thermocycler program, of 2 µl Quantiscript RT buffer 5x, 0.5 µl Quantiscript reverse transcriptase, 0.5 µl Oligo(dT) primer); the thermocycler program used was: 42 °C for 2 minutes, 4 °C pause to add the reverse transcriptase mix as explained before, and manual restart at 42 °C for 30 minutes, 95 °C for 3 minutes and finally 10 °C ∞. Subsequently, we performed the qPCR . Primer sequences were identical to those used by (*Mendoza et al., 2014*). For the qPCR reaction we used a Bio-Rad CFX Connect Real-Time PCR Detection System thermocycler and the Bio-Rad CFX manager software to store and analyze the data. Every sample was run in triplicate in a 96-well plate in a total volume of 10 µl. The mixture contained 5 µl sybrGreen master mix ORA™ qPCR Green ROX H Mix, 2X, from highQu; Table 2.3), 0.5 µl from each primer, 1 µl of 1:10 diluted cDNA and 3 µl sterile H_2O. As reference, we used the housekeeping gene *rp49* (*ribosomal protein 49*), while as a negative control we used the same reaction mix without cDNA. The qPCR thermocycler program used is listed in Table 2.7. The experiments were repeated 2 to 4 times.

2.7 Behavior

All behavioral experiments were performed in Buridan's paradigm (RRID: SCR_006331). In this experiment, we analyzed both temporal components of walking behavior (often subsumed under 'general locomotion') and spatial components such as fixation of landmarks or the straightness of the walking trajectory. Buridan's paradigm (Fig. 7A) consists of a round platform with a diameter of 117 mm which is surrounded by a water-filled moat. The platform is situated at the bottom of a uniformly illuminated white cylinder, 313 mm in height and 293 mm in diameter (*Colomb et al., 2012*). Two black stripes are placed on the inside of the cylinder, opposite to each other, serving as the only visual cues for the flies. Two days-old female flies were collected and their wings were clipped under CO_2 anesthesia. After one night recovery at 25 °C they were tested in Buridan's paradigm for 15 minutes (doi.org/10.17504/protocols.io.c7vzn5). The position of the fly is recorded by a camera (Logitech Quickcam Pro 9000) connected to a computer running our BuriTrack software (http://buridan.sourceforge.net). The analysis software

CeTrAn (*Colomb et al., 2012*) (https://github.com/jcolomb/CeTrAn/tree/master/CeTrAn) extracts a variety of parameters from the sored trajectories. From the parameters extracted by CeTrAn, we used the temporal parameters median speed, distance travelled, number of walks and activitytime and the spatial parameters stripe deviation and meander. It furthermore traces occupancy plots. Around 10 to 20 flies were analyzed per genotype. For the experiment involving *Tub-Gal80ts* (Fig. 3.13C-F), flies were raised at 18 °C, moved to 30 °C for 12 hrs (embryos) or 48 hrs (pupae and adults) and subsequently left at 25 °C for the rest of the development (embryos and pupae) or overnight for recovery (adults) before testing.

2.8 Statistical analysis

All graphs were created and statistical analysis was performed using GraphPad Prism 6 (GraphPad Software, Inc., California, USA) (RRID: SCR_002798) software. The variances were compared with an F-test: where the variances were considered equal we used a Student's t-test (two-tailed) or one way ANOVA followed by Tukey's post hoc test, where they were instead considered significantly different ($p<0.005$) we used a Mann-Whitney U-test or a Kruskal-Wallis followed by Dunn's post hoc test. The initial behavioral experiments (Fig. 3.8) were carried out with a sample size which, from experience, would be sufficient to detect medium to large effects, i.e., N~20. We then used these results to perform a power analysis for the subsequent experiments. We found that effect sizes such as those exhibited in the speed, meander or stripe fixation parameters required a sample size of up to 18 to reach 80 % statistical power at an alpha of 0.5 % (*Benjamin et al., 2018*), while effects such as those in the activity time parameter would require up to 100 flies. We corroborated these analyses with Bayesian analyses, where the activity time parameter yielded a Bayes factor of below one, while the other effects yielded Bayes factor values beyond 100. Therefore, we set the target sample size for all subsequent Buridan experiments to 18 and $p<0.005$ was considered significant. Data are expressed as averages ± SEM or averages ± SD and each case is indicated in the legend of each figure.

Genotype	Usage
;;;ok107-Gal4	driver line
;;ato-Gal4	driver line
;;C380-Gal4	driver line
;;cmpy-Gal4	driver line
;;D42-Gal4;	driver line
*;;FoxP-/-; **	mutant
*;;FoxP-iB-Gal4; **	driver line
*;;FoxP-LexA; **	driver line
;;Tdc2-Gal4;	driver line
*;;UAS-t:gRNA(4xFoxP); **	effector line
;ELAV-Gal4;;	driver line
;LexAop-mCD8-RFP/UAS-mCD8-GFP;;	effector line
;LexAop-Stinger-GFP;;	effector line
;UAS-Cas9;;	effector line
;UAS-CD8-GFP;;	effector line
;UAS-Stinger-GFP;;	effector line
;Vas-Cas9;	mutant
CS-TZ	wild type strain
ELAV-Gal4;Tub-Gal80ts;;	driver line
$FoxP^{3955}$	mutant
Integrase(x);;AttP2	mutant
w-;; D3/TM3, Sb	mutant
white-/-	mutant
WTB	wild type strain

Table 2.1: Complete list of the fly lines used in this study

Step	Temperature	Time	Nr. of Cycles
Denaturation	98 °C	30 s	
Denaturation	98 °C	10 s	
Annealing	60 or 65 °C	30 s	
Elongation	72 °C	60 s	GoTo step 2 x 30
Elongation	72 °C	2 min	
Storage	10 °C	∞	

Table 2.2: PCR program for Phusion and Q5-HF polymerases

Component name	Company	Catalog number
Cutsmart buffer	New England BioLabs	B7204S
LSB buffer	Made in our lab	/
NEB 2.1 buffer	New England BioLabs	B7202S
NEBuilder HiFi DNA Assembly Master Mix	New England BioLabs	E2621L
Phusion polymerase	Made in our lab	/
Phusion polymerase buffer	Made in our lab	/
Q5 polymerase HF	New England BioLabs	M0491S
Q5 polymerase buffer	New England BioLabs	B9027S
Restriction ezymes	New England BioLabs	R0*xxxx*
T4 DNA ligase	ThermoFisher Scientific	EL0011
T4 Ligation buffer	ThermoFisher Scientific	B69
T4 Polynucleotide kinase	New England BioLabs	M0201S
Taq polymerase	Made in our lab	/
Kit	**Company**	**Catalog number**
E.Z.N.A. Gel Extraction Kit	VWR/Omega	101318-972
OneStep RT-PCR Kit	Qiagen	210212
ORA™ qPCR Green ROX H Mix	highQu	QPD0201
peqGOLD TriFast	VWR	30-2010
Qiafilter Midi-Kit	Qiagen	12245

Table 2.3: Complete list of the components and kits used in this study

Step	Temperature	Time	Nr. of Cycles
Denaturation	95 °C	5 min	
Denaturation	95 °C	25 s	
Annealing	50 or 60 °C	30 s	
Elongation	72 °C	60 s	GoTo step 2 x35
Elongation	72 °C	10 min	
Storage	10 °C	∞	

Table 2.4: Colony PCR program for Taq polymerase

Antigen	Host	Dilution	Incubation	Source	RRID
Chaoptin-11	mouse	1:500	1 night	Developmental Studies Hybridoma Bank	AB_528161
ChAT	mouse	1:250	1 night	DSHB	AB_528122
ELAV	rat	1:100	1 night	DSHB	AB_528218
FoxP	guinea pig	1:200	2 nights	Lawton et al., 2014	/
GABA	rabbit	1:250	2 nights	GeneTex	AB_2037030
nc82	mouse	1:500	1 night	DSHB	AB_2314866
p-SMAD1/5	mouse	1:250	2 nights	Cell Signaling	AB_491015

				Technology	
REPO	mouse	1:500	1 night	DSHB	AB_528448
TH	rabbit	1:500	1 night	Millipore	AB_390204

Table 2.5: Complete list of the primary antibodies used in this study

Antigen	Host	Dilution	Incubation	Source	RRID
Alexa-Fluor-Anti-mouse 555	goat	1:250	5 hours	ThermoFisher Scientific	AB_2535844
Alexa-Fluor-Anti-rabbit 555	goat	1:250	5 hours	ThermoFisher Scientific	AB_2535849
Alexa-Fluor-Anti-rat 555	goat	1:250	5 hours	ThermoFisher Scientific	AB_2535855
Anti-guinea pig Cy™3	goat	1:200	7 hours	Jackson ImmunoResearch	AB_2337423

Table 2.6: Complete list of the secondary antibodies used in this study

Step	Temperature	Time	Nr. of Cycles
Denaturation	95 °C	2 min	
Denaturation	95 °C	10 s	
Annealing	60 °C	10 s	
Elongation, measurement	65 °C	30 s	GoTo step 2 x39
Denaturation	95 °C	10 s	
Melting curve, measurement	65 °C – 95 °C	+ 0.5 °C / 5s	

Table 2.7: qPCR program

3. Results

All raw data are publicly accessible with an Attribution 4.0 International (CC BY 4.0) license at https://figshare.com.

On the following results we based a Research Paper soon to be available on *Open Biology* (https://royalsocietypublishing.org/journal/rsob).

3.1 FoxP-isoB expression in the Drosophila brain

The WT FoxP gene is a transcription factor that binds the DNA thanks to FH domain (Fig. 3.1A, yellow boxes); the gene is built by 7 introns and 8 exons (1-8), and the DNA binding domain lies in exon 6, exon 7 and exon 8. Those last two exons are subjected to alternative splicing to originate different protein isoforms: an isoform A (iA) which results from the coupling of exon 6 with exon 7, an isoform B (iB) which instead carries exon 8, and an isoform IR (iIR) which results from the translation of exon 6 and the translation of the first part of the subsequent intron. While the first two isoforms contain a complete and functioning DNA binding domain (with a difference between the two sequences of only 10 amino acid (Fig.3.1A, dashed box)), the IR results to be truncated due to the presence of a stop codon in the intron sequence (Fig. 3.1A, red line), making unlikely for it to exploit the function of the transcription factors. Of the three FoxP isoforms, iB was most directly associated with the learning phenotype discovered by (*Mendoza et al., 2014*). Therefore, we inserted the sequence of the yeast transcription factor Gal4 (driver component of the UAS/Gal4 binary system) into exon 8, which is exclusive to iB (Fig. 3.1A). This insertion leads to the expression of the Gal4 transcription factor only in FoxP-iB positive cells. At the same time, the insertion also disrupts the forkhead-box (FH) DNA binding domain of the FoxP gene, preventing the FoxP protein to act as a transcription factor, effectively mutating the gene for this function. Consequently, we tested for Gal4 reporter gene expression and FoxP expression levels (Fig. 3.1). Observing Gal4 expression with different green fluorescent proteins (GFPs) under control of the UAS promoter (to which Gal4 binds), revealed that FoxP-iB is expressed throughout the whole development of the fly, from embryo (Supplemetary Fig. S1) to adult, in both brain and ventral nerve

cord (VNC) (Fig. 3.1B). In 3rd instar larvae we can clearly see expression in the central brain (but not in the optic lobes) and in the VNC, while in the adult the main expression domains in the neuropil comprise protocerebral bridge, gnathal ganglia (subesophageal zone), vest, saddle, noduli, and superior medial protocerebrum. GFP-positive cell body clusters could be found in the cortex of both the central brain and around the optic lobes (Fig. 3.1B). We next validated the expression pattern of our iB-specific driver line to the staining of an available isoform unspecific polyclonal antibody (*Lawton et al., 2014*). We observed complete colocalization of the driver line with the antibody staining in both larvae and adults, i.e., there were no GFP-positive cells that were not also labeled by the FoxP antibody (Fig. 3.1C). The cells only stained for the FoxP antibody and not for GFP are presumably cells expressing the other FoxP isoforms (iA and iIR, Fig. 3.5). Notably, in contrast to previous reports (*DasGupta et al., 2014; Groschner et al., 2018*) but consistent with (*Castells-Nobau et al., 2019*), we did not detect any FoxP expression in mushroom body cells, neither with our driver line, nor with the antibody.

Postulating that our transgene disrupted expression of FoxP gene, we measured mRNA levels of all three isoforms with RT-qPCR (Fig.3.1D). With one of the primers placed over the Gal4 insertion site, we observed approximately half the wild type FoxP-iB expression levels in heterozygous animals, while FoxP-iB expression was nearly abolished in the homozygous transgenes. We did not observe any change in the other two isoforms in neither hetero- nor homozygous mutants.

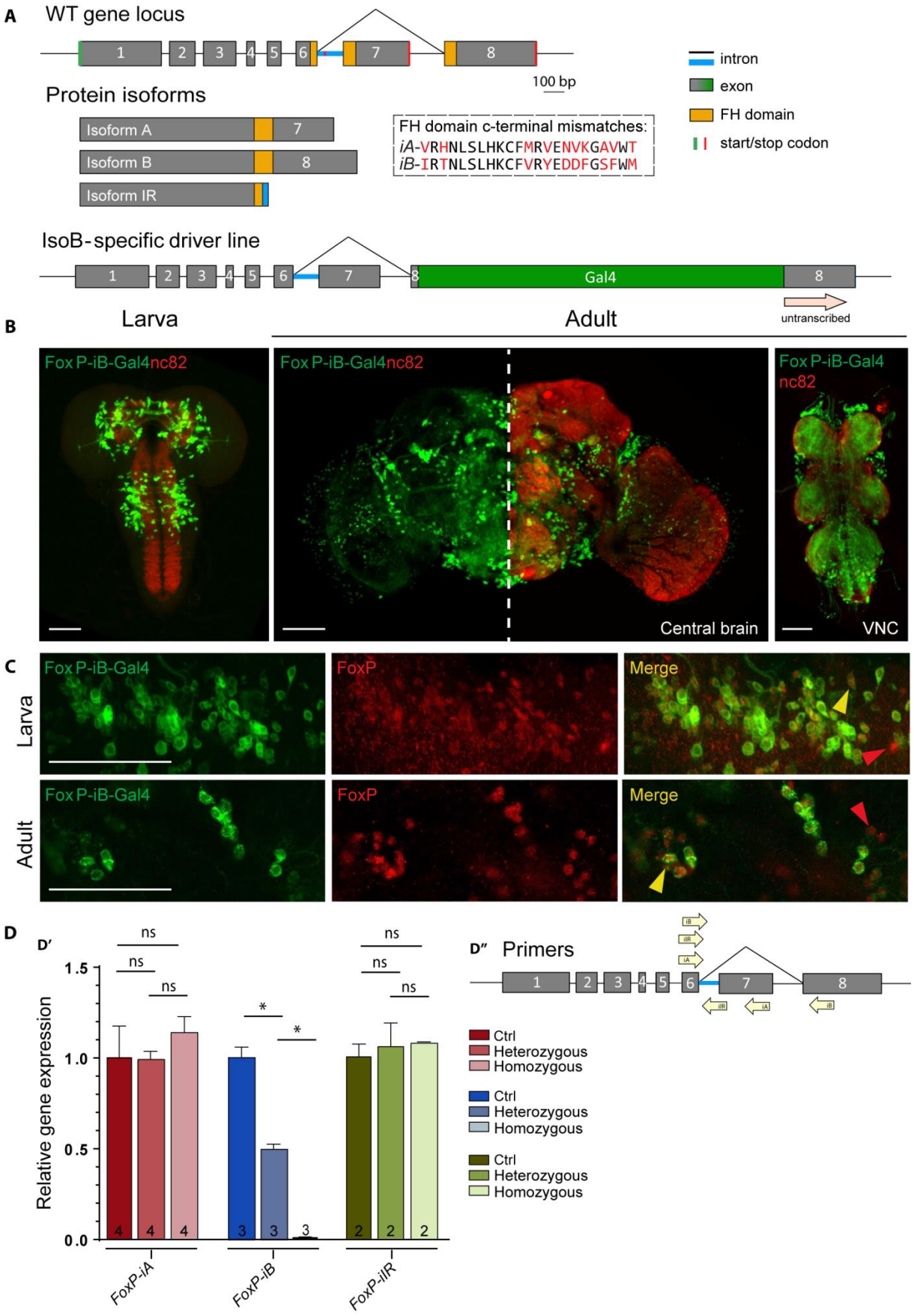
A
WT gene locus
1
2
3
4
5
6
7
8
100 bp
intron
exon
FH domain
start/stop codon
Protein isoforms
Isoform A
Isoform B
Isoform IR
FH domain c-terminal mismatches:
iA-VRHNLSLHKCFMRVENVKGAVWT
iB-IRTNLSLHKCFVRYEDDFGSFWM
IsoB-specific driver line
Gal4
untranscribed
B
Larva
Adult
Fox P-iB-Gal4nc82
Central brain
VNC
C
Larva
Adult
Fox P-iB-Gal4
FoxP
Merge
D
D'
Relative gene expression
ns
*
FoxP-iA
FoxP-iB
FoxP-iIR
D" Primers
Ctrl
Heterozygous
Homozygous

Fig. 3.1: *FoxP-iB expression in the Drosophila nervous system*. (A) Schematic representation of the FoxP gene locus before (above) and after (below) insertion of a Gal4 sequence into exon 8. (B) *FoxP-iB-Gal4>CD8-GFP* expression pattern costained with nc82 in 3rd instar larvae, adult brain and adult VNC. (C) Driver line costained with a polyclonal FoxP antibody in larval and adult brain. The yellow arrowheads indicate colocalization, while the red ones indicate cells only positive for the antibody staining. (D') RT-qPCR for FoxP-iA, iB and IR on controls and hetero and homozygous *FoxP-iB-Gal4* mutant. (D'') Primers used for the RT-qPCR. Data are expressed as means ± SEM. *p<0.005. Scale bars: 50 μm.

3.2 FoxP-isoB is expressed in different types of neurons

With *FoxP* involved in learning and expression patterns suggesting neuronal expression (Fig. 3.1), we investigated whether the observed expression was exclusively neuronal, or if there were also *FoxP-iB* expressing glial cells. Therefore, we stained 3rd instar larva and adult brains with antibodies against ELAV (neuronal marker) and REPO (glial marker). At both developmental stages, the two stainings reveal exclusive *FoxP-iB*-mediated GFP colocalization with ELAV without any colocalization with REPO (Fig. 3.2), suggesting that *FoxP-iB* is expressed exclusively in neurons. These data are consistent with results published previously (*Castells-Nobau et al., 2019; K. Lawton, 2014*), validating the methods employed here.

We next investigated in more detail the type of neurons in which FoxP is expressed (Fig 3.3). Using a variety of antibodies used as markers for different neuronal cell types we detected FoxP-iB expression in most of the cell types investigated. Except for the anti-TH, all of the antibodies used here proved to be working better in the larval nervous system, so we mostly analyzed 3rd instar larvae. Extensive colocalization was observed with p-SMAD1/5 (a motorneuron marker) in the VNC but not in the central brain (CB). Some FoxP-iB neurons were positive for ChAT (cholinergic) or GABA (inhibitory) both in the VNC and in the CB. These data are consistent with the study performed by *Schatton et al., 2018* in honeybees where they found colocalization between AmFoxP positive neurons and GABAergic, cholinergic and monoaminergic markers. Finally, a few FoxP-iB positive neurons were found to colocalize with Tyrosine hydroxylase (dopaminergic neurons) in the CB only. No colocalization was found between FoxP-iB and Chaoptin (a marker for photoreceptor neurons; *Pollock et al., 1990*) (Fig. 3.4).

We also crossed the FoxP-LexA line (see Results section 3.3) with *LexAop-RFP-UAS-CD8-GFP* and *Tdc2-Gal4* to investigate any potential tyraminergic or octopaminergic FoxP neurons, but despite a close proximity between the two cell types, no colocalization was found (Fig. 3.4).

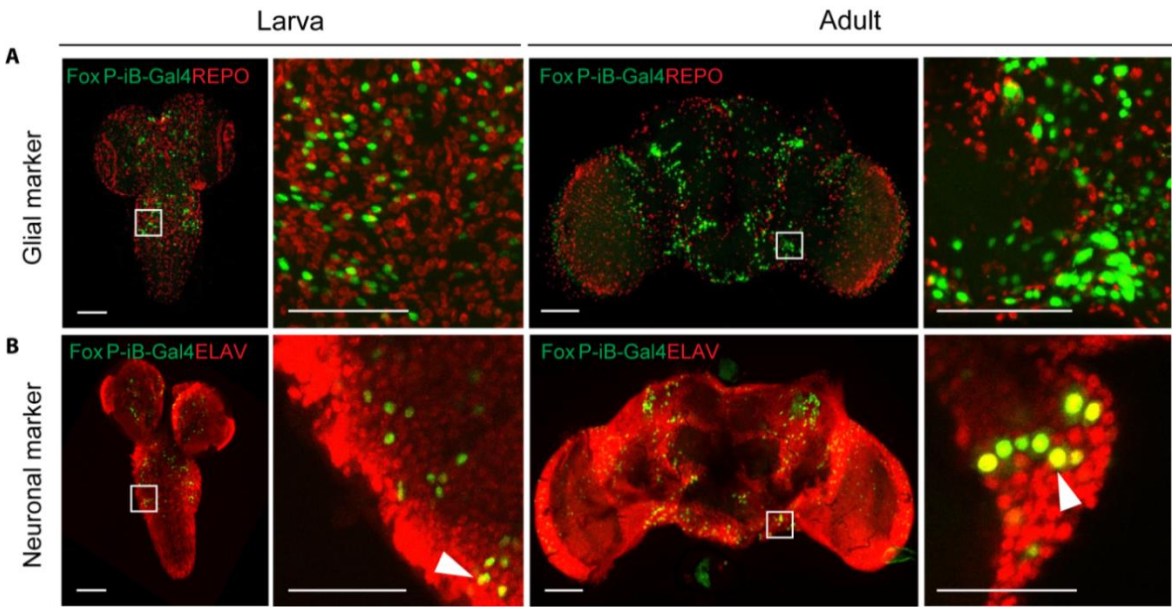

Fig. 3.2: *Only neurons, not glia, are expressing* FoxP-iB *in the Drosophila brain.* Immunohistochemistry on *FoxP-iB-Gal4>Stinger-GFP* flies with REPO (glia, A) and ELAV (neurons, B) markers. Note the lack of colocalization of FoxP-iB driven GFP with the glial marker in both 3rd instar larvae and adult brains (A). In contrast, exclusive colocalization of FoxP-driven GFP with the neuronal marker was observed in both developmental stages (white arrowheads indicate typical examples). Scale bars: 50 µm.

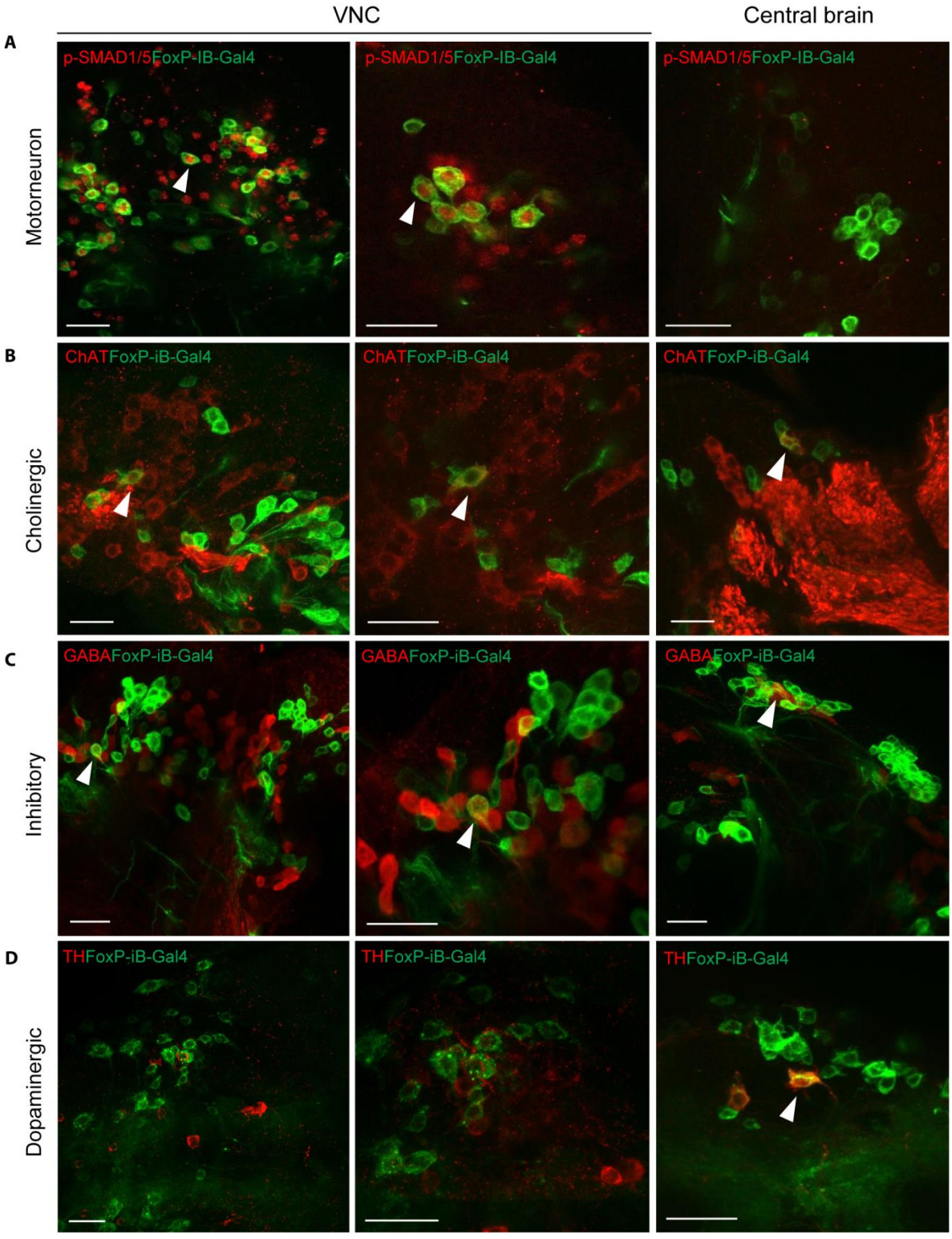

Fig. 3.3: *FoxP-iB is expressed in various types of neurons.* Immunohistochemistry on *FoxP-iB-Gal4>CD8-GFP* flies using different antibodies. (A) Some of the *FoxP-iB* positive neurons colocalize with p-SMAD1/5 in the VNC but not in the central brain. (B-C) *FoxP-iB* neurons positive for ChAT or GABA have been found in both the VNC and CB. (D) Only ew *FoxP-iB* neurons colocalize with TH and only in the CB. White arrowheads indicate examples of colocalization. Scale bars 25 µm.

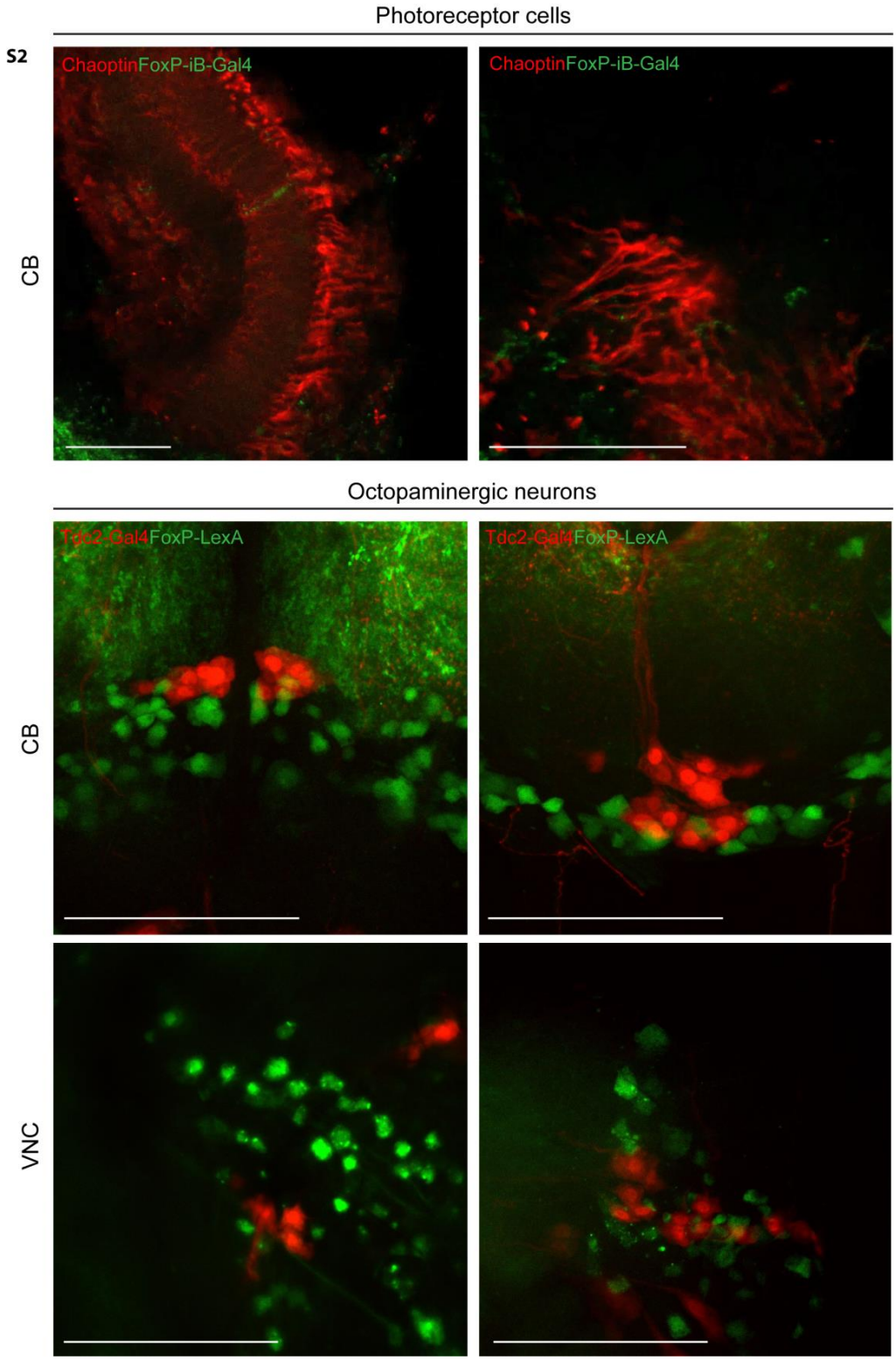

Fig. 3.4*: FoxP-iB is not expressed in photoreceptor or octopaminergic cells*. The immunohistochemistry for a photoreceptor cell marker (upper row) reveal no colocalization between Chaoptin and FoxP-iB. The cross of a *FoxP-LexA* line with *LexAop-RFP-UAS-CD8-GFP* and *Tdc2-Gal4* (two lower rows) show also no colocalization but a great proximity between the two cell types, suggesting a possible communication between the two, in both CB (central brain) and VNC (ventral nerve cord). Scale bars: 50 µm.

3.3 FoxP isoforms are differentially expressed

As the antibody staining against the FoxP protein indicated more cells expressing FoxP than our iB-specific driver line was reporting (Fig. 3.1B), we created a second driver line, designed to drive expression in all FoxP cells, irrespective of isoform. We inserted a sequence for the bacterial LexA transcription factor in exon 3 (Fig. 3.5A), which have a mechanism of action similar to Gal4. Driving *Stinger-GFP* expression with each driver line revealed a more expansive pattern for the isoform unspecific driver (Fig. 3.5B), as the FoxP antibody staining had suggested (Fig. 3.1B). This visual impression was corroborated by a quantification of stained nuclei (Fig. 3.5C). This quantification allowed us to trace the proliferation of FoxP cells from around 500 in 3rd instar larvae to around 1800 in three days-old adults. In contrast, there are only about 300 cells expressing *FoxP-iB* in the 3rd larval instar and around 1300 in three days-old adults. We noticed that the largest differences in terms of cell number between *FoxP-LexA* and *FoxP-iB-Gal4* flies (both larvae and adults) were found in the CB, while the VNC numbers varied considerably less. For instance, in 3rd instar larvae and in three days-old adults, 66 % and 65 %, respectively, of the total number of *FoxP* neurons in the *Drosophila* nervous system express iB. As with our previous insertion, also this one was expected to disrupt expression of the FoxP gene. To investigate the extent of this disruption on the mRNA level, we again performed RT-qPCR. In contrast to the results from our previous insertion, as expected, this insertion affected all isoforms. In heterozygous flies, the expression level was increased, while in homozygous flies it was decreased (Fig. 3.5E). It is important to note that the reverse primers for these isoforms were chosen to target sequences downstream of the insertion site (see Fig. 3.1A).

In order to directly compare the expression patterns of our two driver lines, we used them to drive reporter genes fluorescing at different wavelengths (i.e., *LexAop-RFP;UAS-CD8-GFP*) and analyzed their patterns in adult flies (Fig. 3.6). In this way, we labeled all FoxP-expressing neurons red and neurons that specifically expressed FoxP-iB in green (Fig. 3.6A). We used the "Colocalization Threshold" tool from ImageJ, which computes false colors to enhance the comparison between the two driver lines and let the differences stand out (see M&M) (Fig. 3.6B). We can see that the other two isoforms are expressed also in the antennal lobe, lobula and fan shaped body (Fig. 3.6A, red arrowhead; Fig. 3.6B,

blue areas). Since this las mutant results homozygous for the mutation for FoxP-iB, it is important to mention that, as control, we performed a cell count on both heterozygous and homozygous *FoxP-iB-Gal4* mutants, in order to identify any cell loss in the latter, but no significant change was encountered (Fig. 3.7).

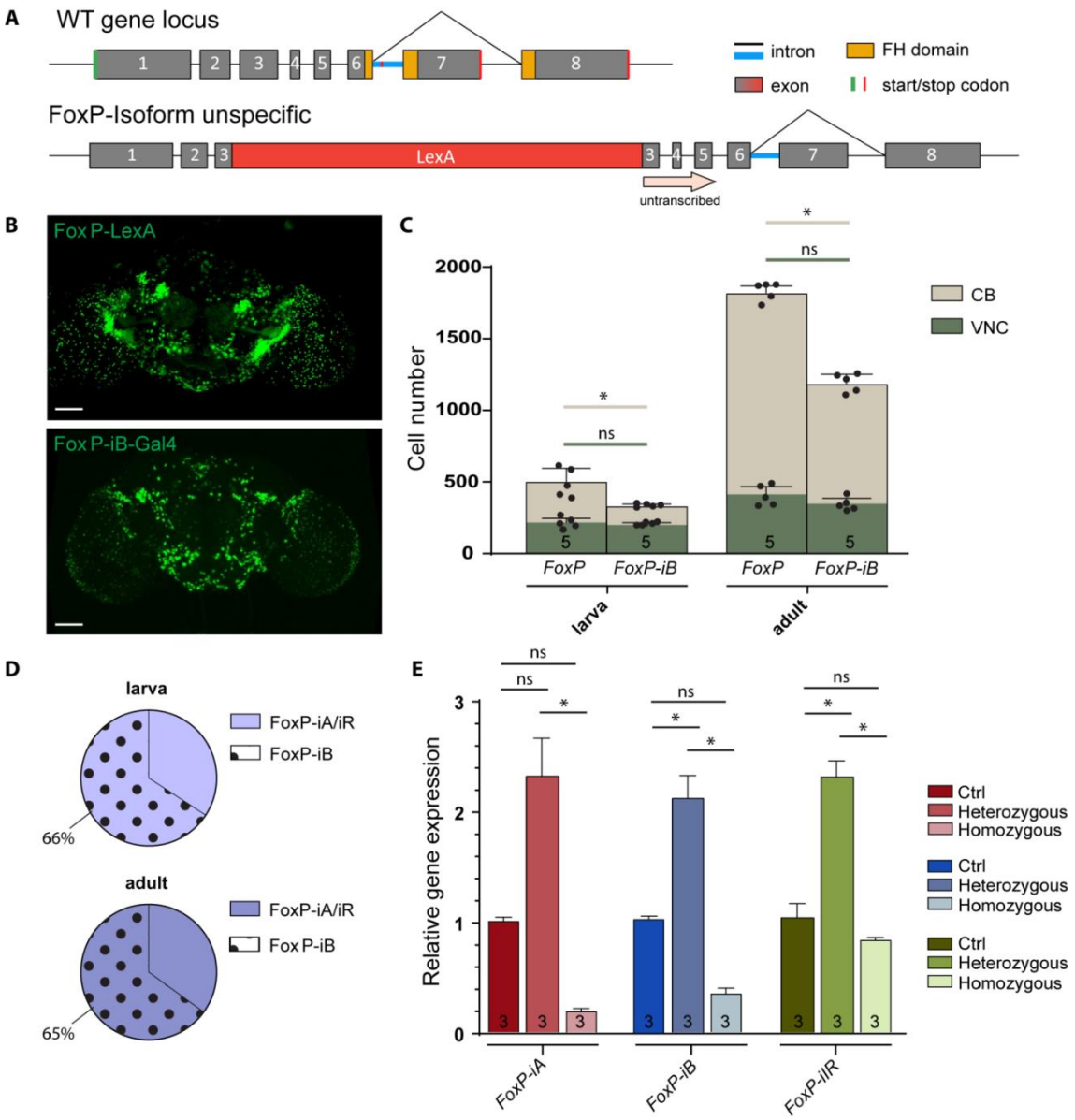

Fig. 3.5: *FoxP-iB is expressed in a subset of FoxP-expressing neurons.* (A) Schematic representation of the FoxP gene locus after LexA insertion. This is an isoform unspecific construct with the insertion of a LexA sequence in exon 3. (B) Expression pattern of *FoxP-LexA* and *FoxP-iB-Gal4* driving *Stinger-GFP*. (C) Cell counting performed with IMARIS on FoxP-LexA and *FoxP-iB-Gal4>Stinger-GFP* (3rd instar larvae and 3 days-old adults) in both CB and VNC. (D) Pie charts that summarize the results from (C). (E) RT-qPCR on *FoxP-LexA* flies (control, hetero- and homozygous flies). Data are expressed as means ± SD in (C) and as means ± SEM in (E). *p<0.005 Scale bars: 50 μm.

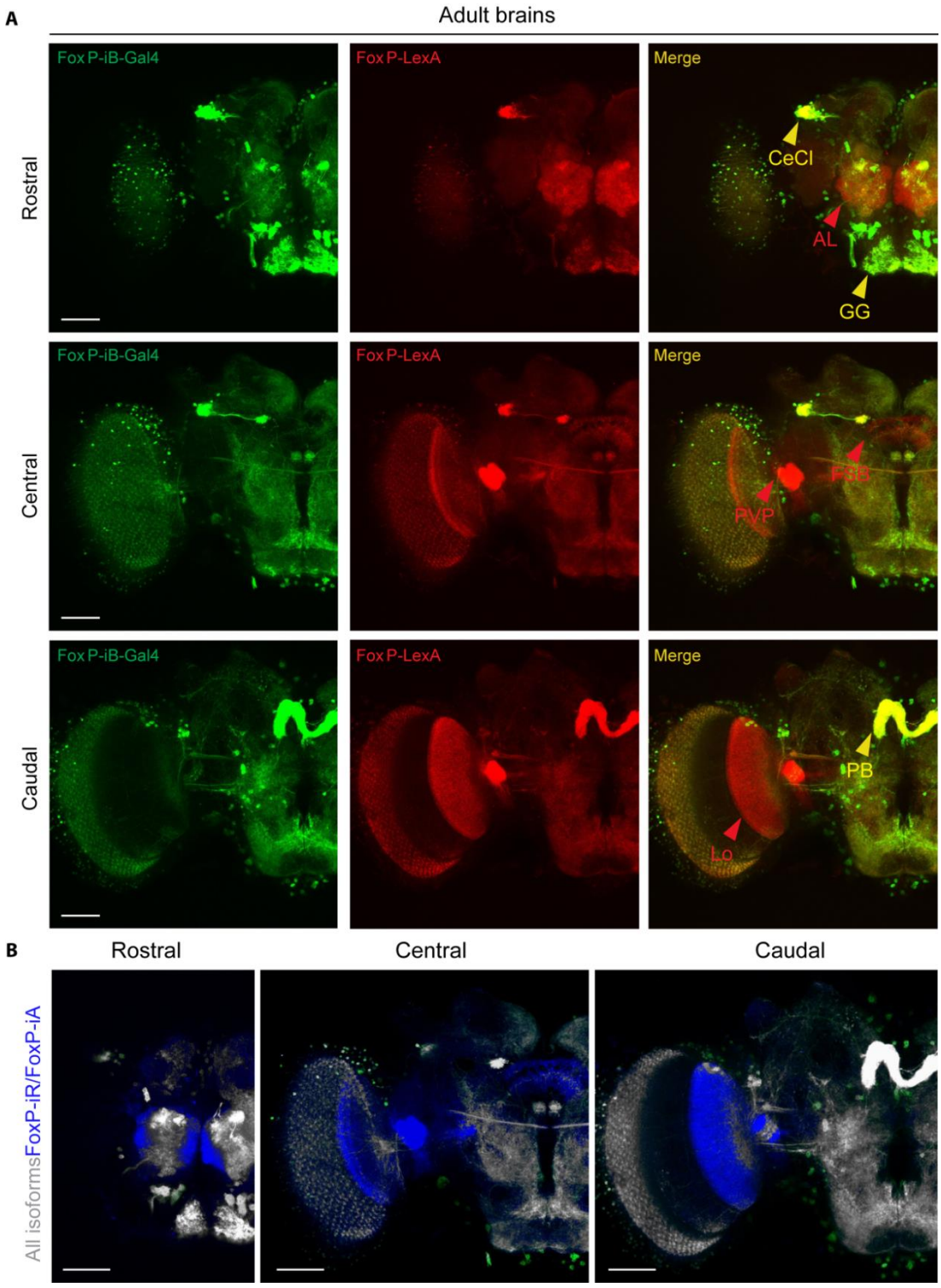

Fig. 3.6: *FoxP-iB expression pattern compared to the one of FoxP.* (A-B) Confocal images of 3rd instar larva and adult brains that express *FoxP-iB-Gal4>CD8-GFP* (green) and *FoxP-LexA>CD8-RFP* (red) together. The image shows in green the areas that express FoxP-iB, in red the total FoxP expression in the Drosophila brain (AL: antennal lobe, PVP: posterior ventrolateral protocerebrum, FSB: fan shaped body, Lo: lobula) and in yellow the areas that are staind by both the construct (CeCl: cell cluster, GG: gnathal ganglion, PB: protocerebral bridge). Scale bars: 50 µm.

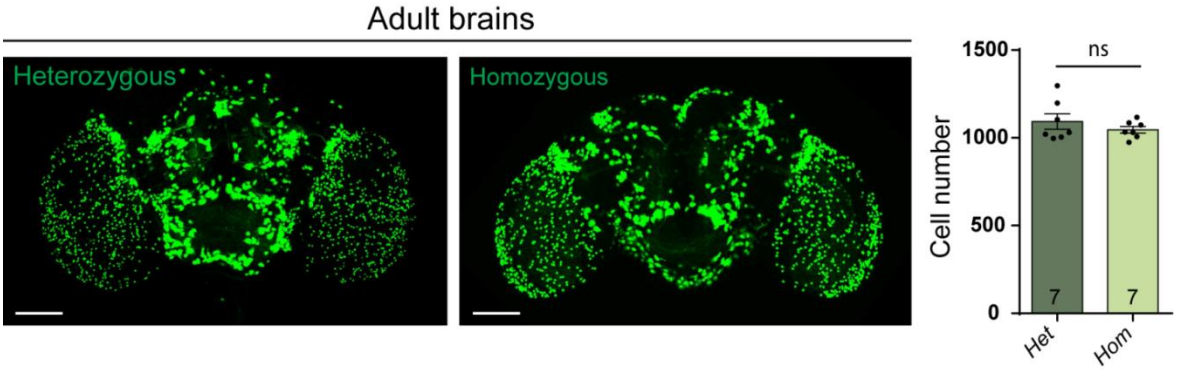

Fig. 3.7: *There is no cell loss in homozygous mutants for FoxP-iB.* A cell count performed on both heterozygous and homozygous mutants for FoxP-iB show that there is no significative difference in cell number, thus no cell loss in homozygous mutants.

3.4 FoxP-isoB knockout flies are impaired in locomotor behavior

Mutations in the FoxP gene do not only affect operant self-learning. For instance, different alleles also affect flight performance and other locomotion behaviors to different degrees (*Castells-Nobau et al., 2019; Lawton et al., 2014; Mendoza et al., 2014*). Because of the FoxP pleiotropy affecting various innate motor behaviors independently from motor learning, we turned to Buridan's paradigm (*Colomb et al., 2012; Götz, 1980*) as a powerful tool to measure several locomotor variables. Buridan's paradigm allows us to test a broad panel of behavioral parameters covering both temporal parameters such as speed or general activity time and spatial parameters such as the straightness of a fly's trajectory (meander) or the degree to which the animal is heading towards one of the two vertical landmarks (stripe fixation), (Fig. 3.8A). With our insertions constituting novel alleles impairing FoxP expression (Figs. 3.1, 3.4), we started by testing the heterozygous and homozygous driver strains without any effectors. Consistent with previous findings of impaired locomotor behavior in FoxP manipulated flies (*Castells-Nobau et al., 2019; Lawton et al., 2014; Mendoza et al., 2014*) and the qPCR results showing reduced FoxP expression (Fig. 3.1D), our *FoxP-iB-Gal4* insertion shows abnormalities in Buridan's paradigm both in temporal as well as in spatial parameters (Fig. 3.8). While the homozygous flies walked more slowly, spent more time at rest and fixated the stripes less strongly than wild type control flies, heterozygous flies did not show the same trend. While in general the differences to wild type flies were less pronounced than for homozygous flies, the temporal parameters tended generally towards the other direction, i.e., the heterozygous flies tended to be faster and

more active than wild type controls, leading to significantly more distance traveled during the experiment (Fig. 3.8B). In contrast, for the temporal parameter stripe deviation (a quantification of stripe fixation, Fig. 3.8C), the heterozygous flies come to lie between homozygous mutants and wild type controls. Thus, this FoxP allele exhibits differential dominance: recessive (or intermediate) in some phenotypes and overdominant in others. Overall, however, the differences between wild type controls and heterozygous flies were much less dramatic than those between wild type flies and homozygous insertions. With different effect sizes in each parameter, we selected two representative parameters for the temporal and the spatial domain, respectively, for comparison of all subsequent lines: walking speed, activity time, meander and stripe fixation. Examples of single trajectories travelled by the flies can be seen in Supplementary Fig. S2 (upper row).

Because our insertion is located in the same exon as the insertion in the *FoxP3955* mutant, we tested the FoxP3955 mutant flies in Buridan's paradigm and found changes in several temporal parameters, similar to those observed in our driver line (Fig. 3.8D). However, meander and stripe fixation appear unchanged in these flies. Thus, besides the deficits in operant self-learning and flight performance as reported previously (*Mendoza et al., 2014*), the *FoxP3955* mutant flies are also deficient in several temporal parameters of walking behavior in Buridan's paradigm. This walking phenotype is consistent with previous findings of walking deficits associated with FoxP manipulations (*Castells-Nobau et al., 2019; Lawton et al., 2014*), but was not detected in a previous publication where walking deficits were tested (*DasGupta et al., 2014*).

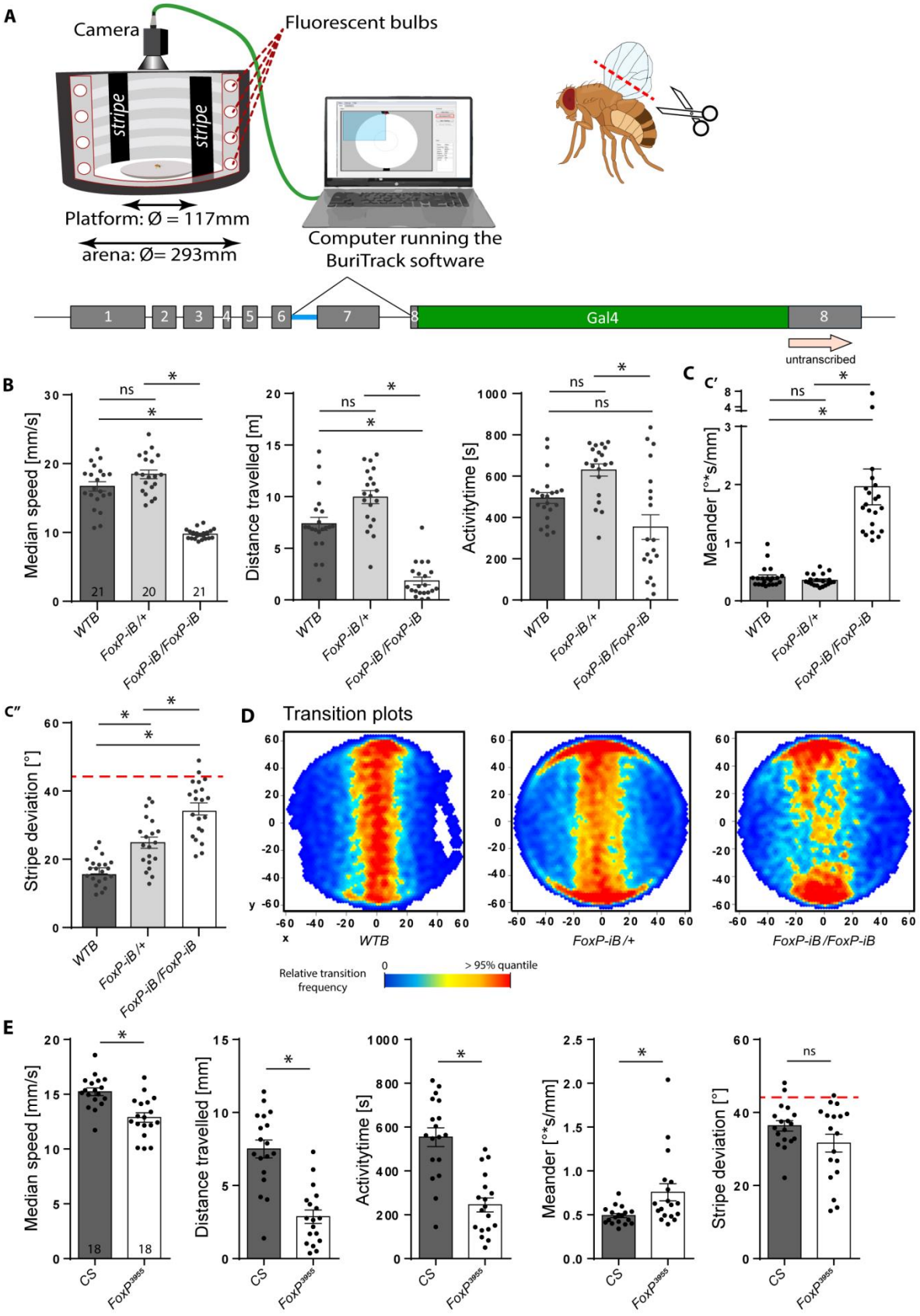
A
Camera
Fluorescent bulbs
stripe
stripe
Platform: Ø = 117mm
arena: Ø= 293mm
Computer running the BuriTrack software
1
2
3
4
5
6
7
8
Gal4
8
untranscribed
B
Median speed [mm/s]
Distance travelled [m]
Activitytime [s]
C
C'
Meander [°*s/mm]
C''
Stripe deviation [°]
WTB
FoxP-iB/+
FoxP-iB/FoxP-iB
21
20
21
ns
*
D
Transition plots
WTB
FoxP-iB/+
FoxP-iB/FoxP-iB
Relative transition frequency
0
> 95% quantile
E
Median speed [mm/s]
Distance travelled [mm]
Activitytime [s]
Meander [°*s/mm]
Stripe deviation [°]
CS
FoxP3955
18
18

Fig. 3.8: *FoxP-iB mutant flies are impaired in several parameters in Buridan's paradigm*. (A) Schematic of Buridan's paradigm. A fly with shortened wings is put in the center of a platform inside a circular arena with two opposing black stripes on the walls. A camera records the position of the fly and the BuriTrack software stores the position data for later analysis with CeTrAn. (B) Temporal parameters. Median speed denotes the instantaneous speed when a fly is walking. Activity time denotes the time spent walking. Distance traveled measures the distance covered by the fly during the experiment. (C) Spatial parameters. Stripe deviation measures the angular deviation from heading towards the center of the stripe to which the fly is oriented. Red dashed line indicates angular stripe deviation of a random walk. (D) The transition plots show the distribution of the platform locations that the flies transitioned through. (E) Buridan's paradigm on CS flies and FoxP3955 mutants. Meander is a measure for the straightness of a fly's trajectory. *$p<0.005$.

3.5 FoxP-all isoform knockout and comparison with FoxP-isoB mutant

With such dramatic motor alterations when only FoxP-iB, which is only expressed in about 65% of all FoxP-positive neurons (Fig. 3.5), is removed (Fig. 3.8) it is interesting to study the effects of removing the remaining isoforms for a complete FoxP knockout. To avoid unwanted potential side-effects of expressing a different protein in its stead, we created a third fly line where the entire second exon is removed together with parts of exons 1 and 3. We validated this mutant with the polyclonal antibody we used before (Fig. 3.1). While the antibody detected the FoxP gene product in control flies, there was no signal in our homozygous knock-out flies (Fig. 3.9A, B). Analogous to the behavioral characterization in the FoxP-iB insertion line, we tested both heterozygous and homozygous FoxP-KO deletion mutants in Buridan's paradigm (Fig. 3.9C-F). The results of this experiment closely resemble the ones from the *FoxP-iB-Gal4* insertion line, with homozygous mutants being both significantly less active (Fig. 3.9C) and fixating the stripes less strongly than the heterozygous mutants and the controls (Fig. 3.9D, E). Also for this allele, the heterozygous FoxP-KO mutants show higher values for all temporal parameters compared to the wild type controls, while there is no difference in stripe deviation. Thus, also the FoxP-KO allele exhibits differential dominance. Examples of single trajectories travelled by the flies can be seen in Supplementary Fig. S2 (lower row).

A direct comparison of the data from the two homozygous alleles (FoxP-iB and FoxP-KO) showed only a small difference in walking speed (Fig. 3.9F), but no significant difference for all the other parameters considered if not just a small trend. Thus, removing the other FoxP isoforms had hardly any effect beyond the consequences of removing only FoxP-iB alone.

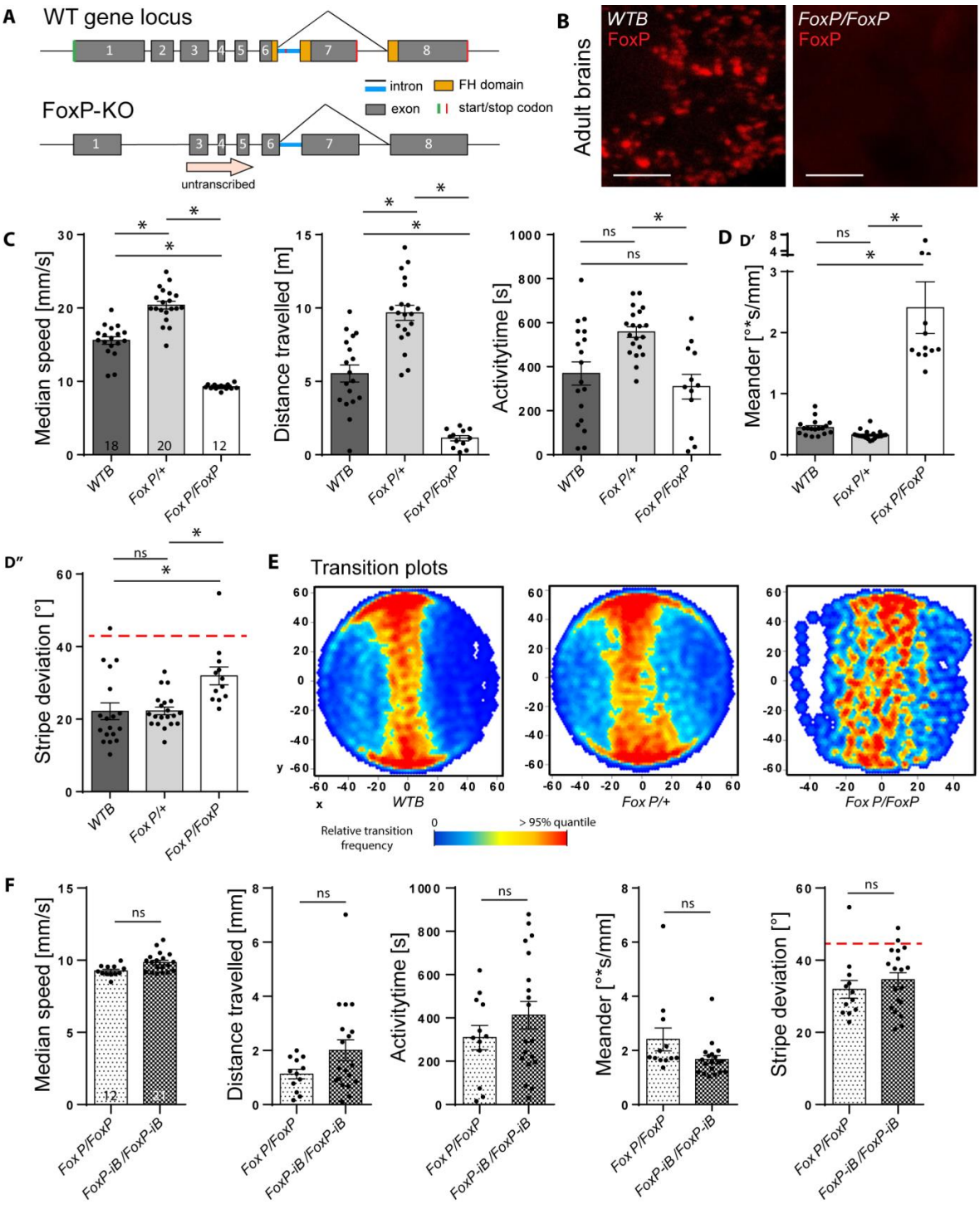

Fig. 3.9: *Deleting the entire FoxP gene has similar consequences in Buridan's paradigm as deleting only FoxP-iB.* (A) Schematic representation of the deletion (*FoxP-KO*) and the wild type (*WT*) gene locus. (B) Immunohistochemistry staining for the FoxP gene product in wild type and *FoxP-KO* mutant brains. (C) Temporal parameters. See Fig. 7 and M&M for definitions. Note the overdominance of the heterozygous *FoxP-KO* flies. Stripe deviation (D) and transition plots (E) show weaker stripe fixation of homozygous FoxP-KO flies. (F) Comparing *FoxP-KO* and *FoxP-iB* flies reveal only a small difference in walking speed. *p<0.005. Scale bars: 25 µm.

3.6 Area-specific conditional FoxP knockout

Given the patchy expression pattern of FoxP in the fly's nervous system (Figs. 1-6) and the grave consequences for behavior in Buridan's paradigm if it is manipulated, we sought to investigate when and where FoxP is required for normal walking behavior. To this end, we designed a fourth fly strain which carries a UAS-controlled effector (Fig. 3.10A). The four guide RNAs (gRNA) each target a different section of the FoxP gene (see M&M). If expressed together with the endonuclease Cas9, this effector efficiently excises the targeted gene (*Port and Bullock, 2016; Xie et al., 2015*). We validated this approach by driving both our gRNAs as well as Cas9 using the pan-neuronal *elav-Gal4* driver and monitoring FoxP expression with the FoxP antibody used before (Fig. 3.10B). Flies with this pan-neuronal excision of the FoxP gene (FoxP-cKO) were also tested in Buridan's paradigm and showed even more severe impairments than flies homozygous for a constitutive deletion of the gene (Fig. 3.10C). In fact, the mutated flies walked so little, that analysis of spatial parameters was not meaningful (Fig. 3.10D).

To allow for temporal control of transgene expression, we also validated the use of the temperature-sensitive suppressor of Gal4, Gal80TS (Fig. 3.10E). The constitutively expressed Gal80TS prevents Gal4 from activating transcription of the UAS-controlled trangenes until the temperature is shifted from 18 °C to 30 °C, at which point the repressor becomes inactivated and Gal4-mediated transcription commences (*McGuire et al., 2003; 2004*). Using this system to drive gRNA/Cas9 expression for 12 hours in the embryo phenocopies both the mutant and the conditional phenotypes not only on the protein (Fig. 8F), but also on the behavioral level (Fig. 3.10G, H). In both experiments, the effects of the manipulations were so severe, that it was not possible to reach the target sample size of 18.

Recently, *Linneweber et al., 2020* described the consequences of silencing dorsal cluster neurons (DCNs) on stripe fixation behavior in Buridan's paradigm. The FoxP-iB expression pattern suggests that at least some of these DCNs express FoxP (Fig. 3.1). Comparing our isoform-unspecific *FoxP-LexA* expression pattern with that of the atonal-Gal4 line used to drive expression in DCNs (*Hassan et al., 2000*) we observed substantial overlap (Fig. 3.11A). Therefore, we use *ato-Gal4* to excise the FoxP gene specifically in DCNs. Interestingly, this manipulation did not have any effect on the flies' behavior in

Buridan's paradigm (Fig. 3.11B). The insect mushroom-bodies (MBs) are not only known as a center for olfactory learning and memory (*Dolan et al., 2018; Felsenberg et al., 2018; König et al., 2019; Lyutova et al., 2019; Thum and Gerber, 2019; Turrel et al., 2018; e.g., Warth Pérez Arias et al., 2020; Widmer et al., 2018*), they are also involved in the temporal and spatial control of locomotor activity (*Besson and Martin, 2005; Helfrich-Förster et al., 2002; Lark et al., 2017; Lebreton and Martin, 2009; Mabuchi et al., 2016; Manjila et al., 2019; e.g., Martin et al., 1998; Serway et al., 2009; Sun et al., 2018; Xiong et al., 2010*). In addition, *Castells-Nobau et al., 2019* found a subtle structural phenotype in a sub-section of the MBs without detectable FoxP expression in the MB Kenyon cells themselves. Finally, there are two reports that expressing anti-FoxP RNAi constructs exclusively in the MBs can have behavioral effects (*DasGupta et al., 2014; Groschner et al., 2018*). For these reasons, despite neither *Castells-Nobau et al., 2019* nor us being able to detect any FoxP expression in the MBs, we excised FoxP from MB Kenyon cells using the *ok107-Gal4* driver and tested the flies in Buridan's paradigm. We did not detect any differences to control flies in these experiments (Fig. 3.11C).

There are two reasons for knocking out FoxP in motorneurons, besides FoxP expression there (Fig. 3.3): first, networks of motorneurons in the VNC control movement patterns and walking is directly affected by our manipulations (Figs. 3.8; 3.9). Second, motorneurons were shown to be important for the type of operant self-learning that also requires FoxP (*Colomb and Brembs, 2016*). Driving expression of gRNA/Cas9 with either of two motorneuron-specific driver lines (*D42-Gal4* and *C380-Gal4*) led to a significant reduction in locomotor activity in Buridan's paradigm, both for spatial and for temporal parameters (Fig. 3.12A, B). Perhaps the most prevalent FoxP expression can be observed in the protocerebral bridge (PB, Fig. 3.1). The driver line *cmpy-Gal4* targets the PCB specifically and drives expression in FoxP-positive neurons (Fig. 3.12C). Removing the FoxP gene exclusively in these neurons led to a significant reduction of locomotor activity (Fig. 3.12D) as well as a reduction in stripe fixation and to more tortuous trajectories (Fig. 3.12E).

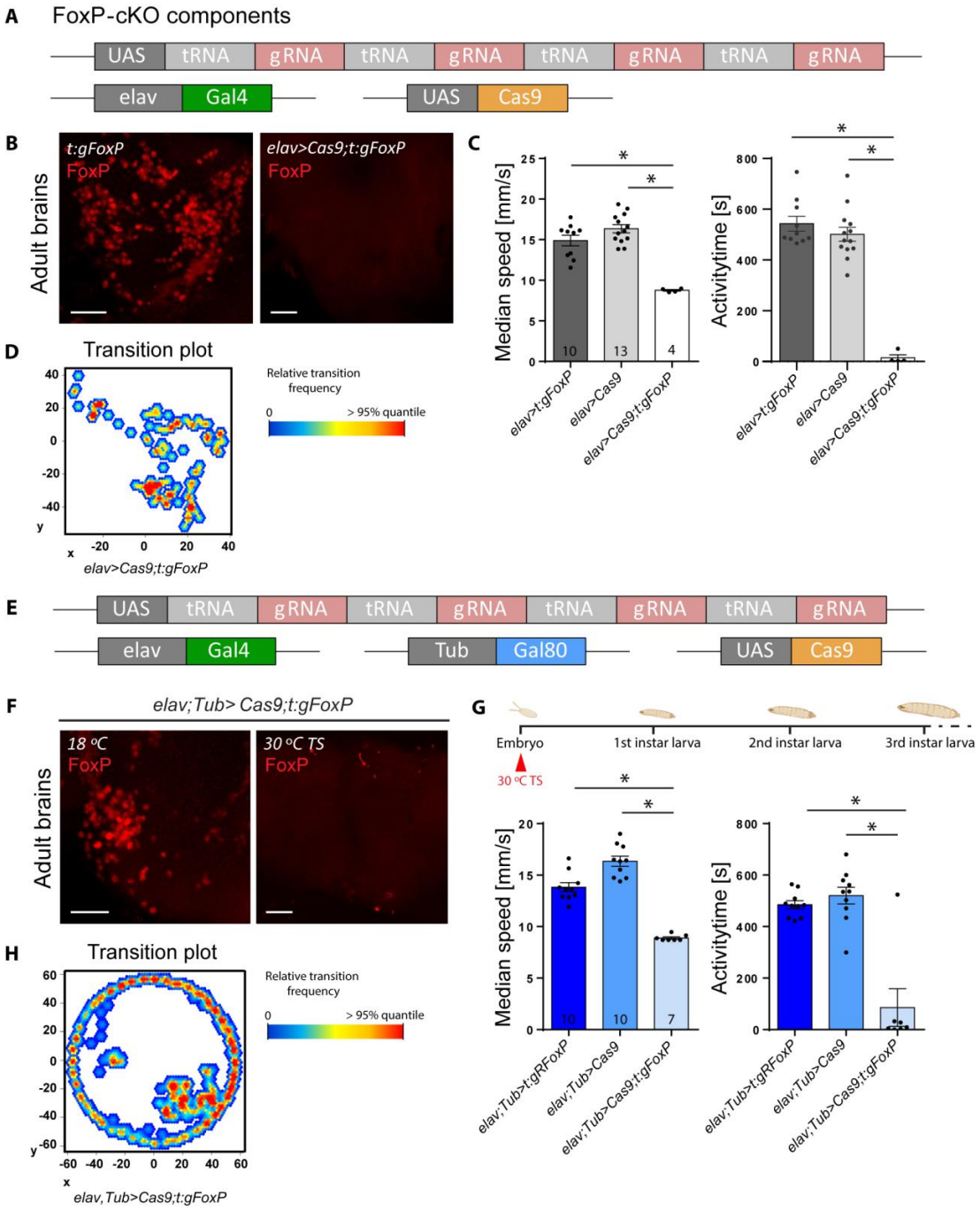

Fig. 3.10: *Conditional FoxP gene knock-out mimics mutant phenotype*. (A) Construct schematic of the effector (UAS) line we created, together with the *elav* driver line and Cas9 effector. (B) Immunohistochemistry on adult brains of the effector control line (left), and of the experimental cross (right). Driving expression of our gRNA construct with *elav-Gal4* leads to a highly efficient FoxP gene knock-out. (C) This knock-out is also validated in Buridan's paradigm, where the experimental flies show strongly reduced locomotor activity. (D) Transition plot showing the reduced activity of FoxP-cKO flies. (E) Schematic of the used transgenic elements. Gal80ts inhibits Gal4 under 30 °C. (F) Induction of panneural gRNA expression in the embryo eliminates FoxP expression as tested with a FoxP antibody (right) compared to uninduced controls (left). (G-H) Inducing panneural gRNA expression in the embryo also leads to similar locomotor defects as observed in mutants and in flies expressing the gRNAs without temporal control. *p<0.005. Scale bars: 25 µm

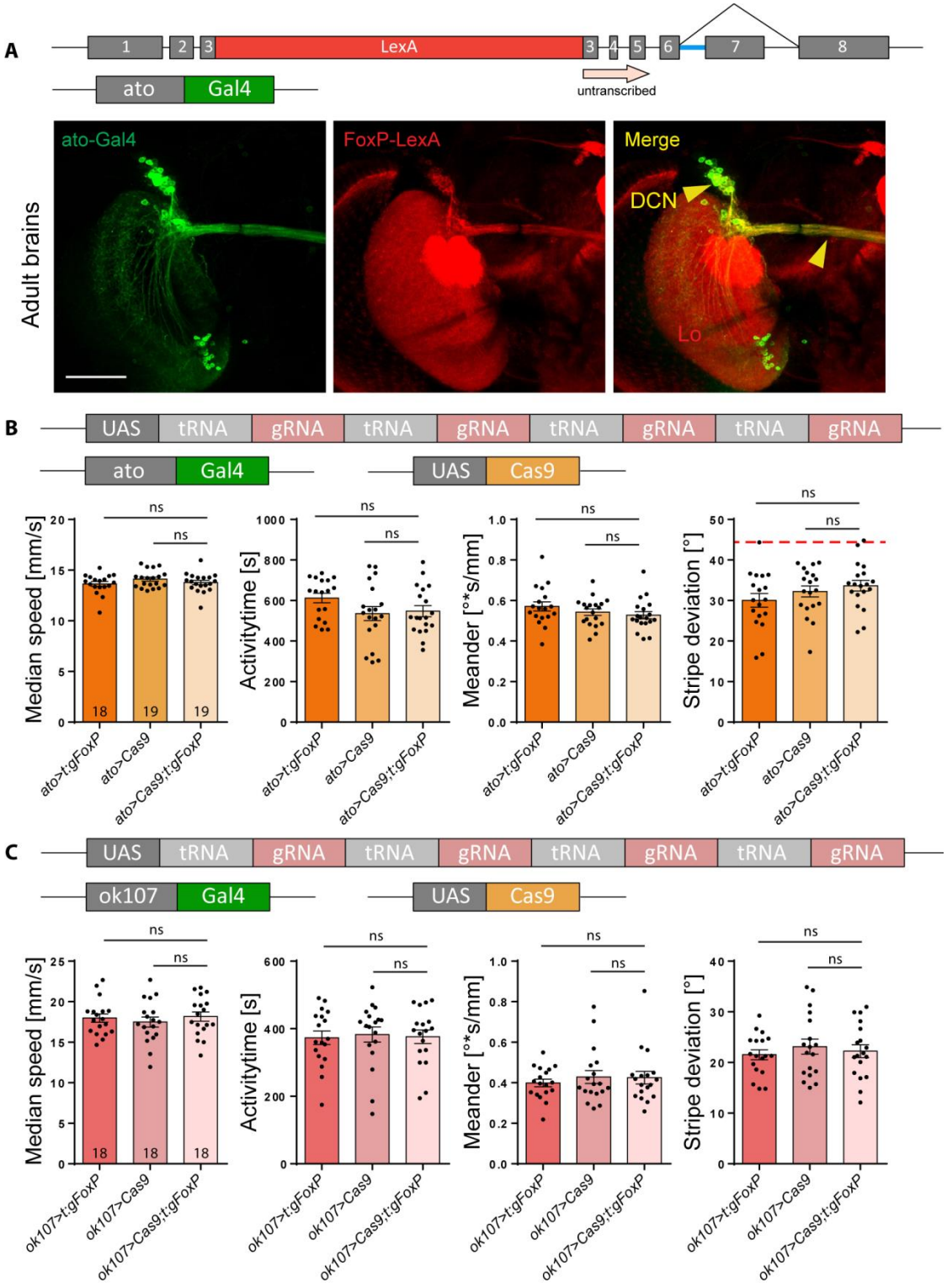

Fig. 3.11: *Conditional FoxP-KO shows no effect in dorsal cluster neurons or mushroom bodies*. (A) Immunohistochemistry showing FoxP-LexA expression in the adult brain compared to the expression of the *ato-Gal4* driver. DCN: dorsal cluster neurons, Lo: lobula, Scale bars: 25 µm. (B) Temporal and spatial parameters from Buridan's experiment show no effects of knocking out the FoxP gene in dorsal cluster neurons using the *ato-Gal4* driver. (C) Knocking out the FoxP gene in the mushroom bodies using the *ok107-Gal4* driver has no effect on either spatial or temporal parameters in Buridan's paradigm.

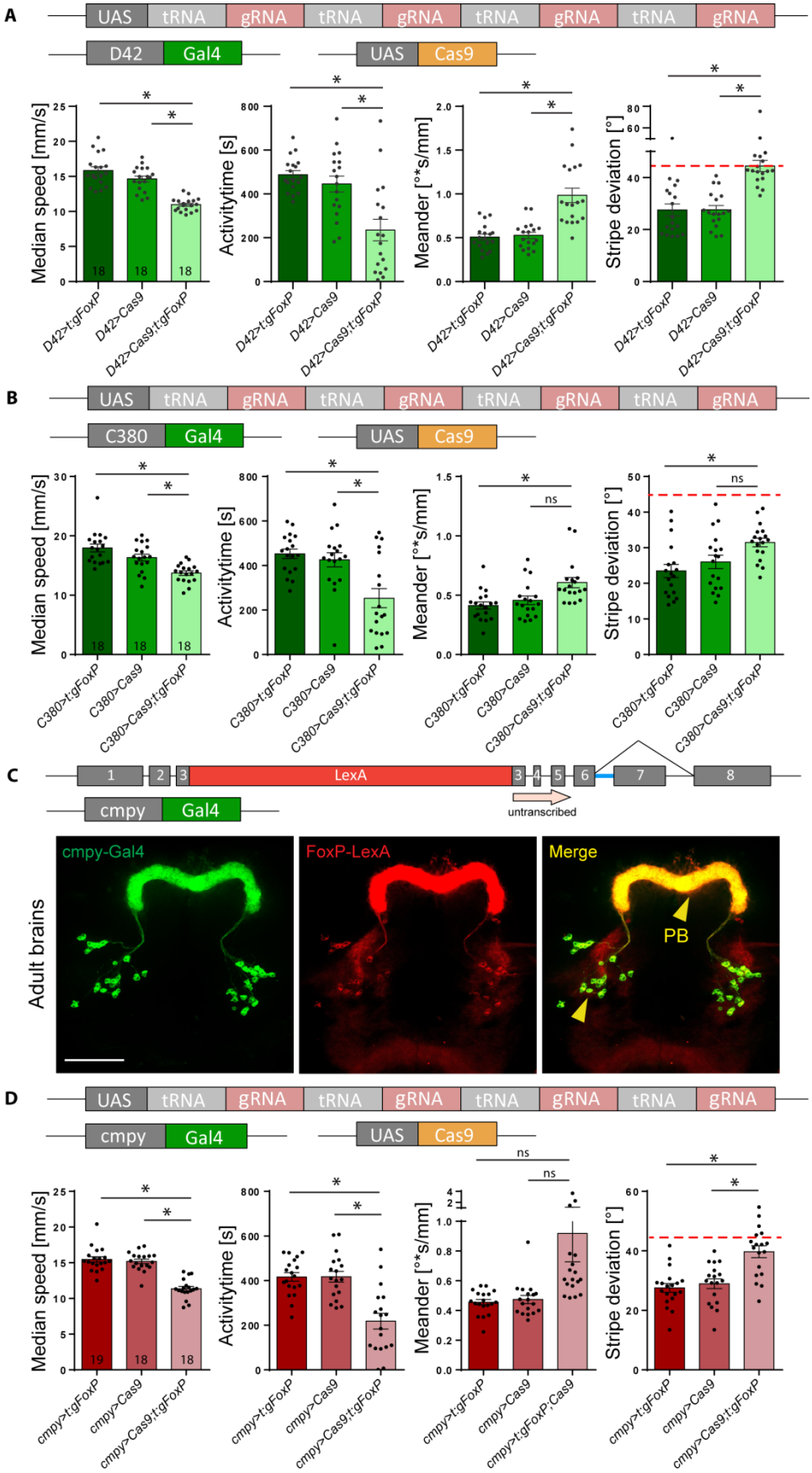
A
UAS
tRNA
gRNA
tRNA
gRNA
tRNA
gRNA
tRNA
gRNA
D42
Gal4
UAS
Cas9
Median speed [mm/s]
Activitytime [s]
Meander [°*s/mm]
Stripe deviation [°]
18
18
18
D42>t:gFoxP
D42>Cas9
D42>Cas9;t:gFoxP
B
C380
Gal4
ns
C380>t:gFoxP
C380>Cas9
C380>Cas9;t:gFoxP
C
1
2
3
LexA
4
5
6
7
8
cmpy
Gal4
untranscribed
Adult brains
cmpy-Gal4
FoxP-LexA
Merge
PB
D
19
cmpy>t:gFoxP
cmpy>Cas9
cmpy>Cas9;t:gFoxP
cmpy>t:gFoxP;Cas9

Fig. 3.12*: FoxP is required in both motorneurons and protocerebral bridge for normal walking behavior in Buridan's paradigm*. (A, B) Both motorneuron-specific driver lines D42-Gal4 (A) and C380-Gal4 (B) show similar reductions in walking speed and activity time, combined with an increase in stripe deviation, indicating poorer stripe fixation. The reduction in activity time for D42 fails to reach statistical significance, apparently due to a low value for the Cas9 control line. (C) The cmpy-Gal4 driver stains an overlapping set of protocerebral bridge (PB) neurons compared to our FoxP-LexA driver line. Scale bars 25 μm (D) Knocking out the FoxP gene in cmpy-Gal4-positive neurons leads to similar alterations in walking behavior in Buridan's paradigm as a complete knock-out, i.e., reduced walking speed, reduced activity time, decreased stripe fixation and increased meander. *$p<0.005$.

3.7 Time-specific conditional FoxP knockout

With *FoxP* being a transcription factor active throughout development and particularly important during pupal development (*Castells-Nobau et al., 2019; Schatton and Scharff, 2017*), we knocked out *FoxP* in all neurons by adding the Gal4 repressor Gal80 to our pan-neuronal *FoxP-cKO* (Fig. 3.13A) and treating the flies with a 48 hrs 30 °C heat treatment during the early pupal stage. This regime did not affect walking behavior in Buridan's paradigm (Fig. 3.13B). Shifting the temperature treatment to immediately after eclosion also did not affect the flies' behavior in Buridan's paradigm (Fig. 3.13C). Taken together, these data indicate that *FoxP* is required for the proper development of, for instance, motor neurons and PCB neurons, but once these circuitries are in place, FoxP expression does not appear to have any immediate mechanistic role in locomotion any more.

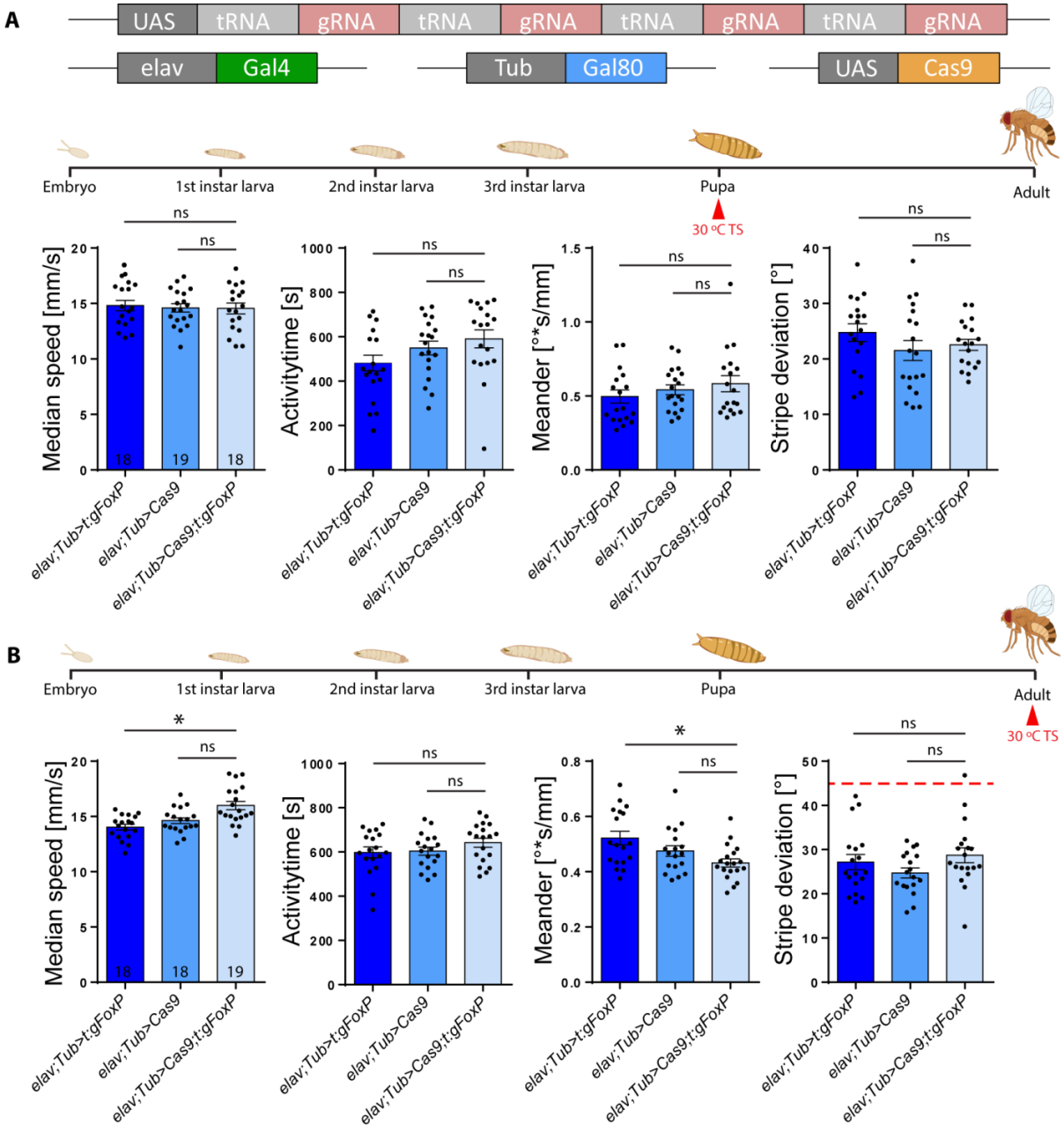

Fig. 3.13: *Adult FoxP expression is not required for normal locomotor behavior in Buridan's paradigm.* (A) Genetic tools used to perform the temporally controlled FoxP knock out. (B) Neither temporal (median speed and activity time) nor spatial (meander and stripe deviation) parameters are altered in adult flies in Buridan's paradigm after inducing the FoxP KO in the early pupa. (C) Neither temporal nor spatial parameters are changed in adult flies in Buridan's paradigm after inducing the FoxP KO immediately after eclosion. *p<0.005.

4. Discussion

4.1 FoxP is expressed in various neuropils and cell-types

The expression pattern of FoxP has been long debated in the last 10 years, nevertheless, each evidence seems to strongly contradict the others. The first published record of a *FoxP-Gal4* expression pattern in *Drosophila melanogaster* is from *Lawton et al., 2014*, where, in addition to the creation of a polyclonal antibody against FoxP, they created a *FoxP-Gal4* line where a 1.5 kb fragment of genomic DNA upstream of FoxP was used as a promoter region for the expression of the Gal4. With this line they were able to describe the expression pattern as a small number of neurons distributed in various areas of the brain, particularly in the PCB. The second published report on FoxP expression pattern in *Drosophila* is from *DasGupta et al., 2014*, where they used a different FoxP promoter fragment (1.4 kb) to direct the expression of a Gal4. What they saw is an expression confined to two subsets of Kenyon cells of the mushroom bodies. Later, *Schatton and Scharff, 2017* created yet another Gal4 line with a FoxP promoter fragment of 1.9 kb. Their larger fragment contained the sequences of the two previously used fragments. They saw again expression in the mushroom bodies amongst other areas. Finally, the last report of a FoxP expression pattern is from *Castells-Nobau et al., 2019*, where they created a line expressing FoxP tagged with GFP using a fosmid vector, where they cloned a GFP sequence downstream of FoxP. Giving the GFP a nuclear signal, even though good cell bodies localization was visible, it was difficult to identify the respective neuropils. Furthermore, besides fruit flies, to complicate the picture, studies on FoxP expression pattern have been carried out during the years also in other insects, like honeybees (*Apis mellifera*), where the situation seems analogously thorny. The first report of an expression pattern in this animal is from *Kiya at al., 2008*, where with an *in-situ* hybridization they detected FoxP expression in particular brain regions such as optic lobe and protocerebral lobe. This description seems to match the one described in flies by *Lawton et al., 2014*. Subsequently *Schatton and Scharff, 2017* described the same expression pattern with the only exception that they also saw expression in the Kenyon cells of the mushroom bodies. In order to shed light on those contradicting evidences, what we do here, is to use two state-of-the-art CRISPR/Cas9 techniques: the Homology Directed Repair (HDR) (*Gratz et al.*,

2014) and the t-RNA based vectors for producing multiple clustered regularly-interspaced CRISPR gRNA from a single transcript (*Port and Bullock., 2016*). Thus, what we propose is a novel kind of mutants that allowed us to act directly in the genomic locus, without disrupting the complex regulation that may occur from distant parts in the genome. It has been shown with the 3C technique (chromatin conformation capture) in fact, that in human cells there are at least 18 different genomic regions that are in physical contact with the *FOXP2* (a *dFoxP* homologous) promoter, some of which act as enhancers (*Becker et al., 2018*). Furthermore, by acting directly in the genomic locus, we avoid the risk that the Gal4 expression might be influenced by position effects exerted by local regulators. Another advantage of these lines that we created (*Gal4* and *LexA* driver lines and *UAS* effector line in particular), is the versatility, which allows us to avoid the confinement given by both the cloning of a GFP sequence directly in the genome of the flies, and by the static non-inducible KO mutants. The expression pattern results we got from our *Gal4* line reveal strong FoxP-iB expression in various neuropil regions: superior medial protocerebrum, protocerebral bridge, noduli, vest, saddle, gnathal ganglia and medulla (summarized in Fig. 4.1A). The *LexA* line reveals instead the expression pattern of all the isoforms of FoxP, and it thus colocalizes in most parts with the *FoxP-iB-Gal4*. There are however, some areas that appear to be only marked by the LexA line, and this thus indicates that those areas express only isoform A and/or IR. Those areas are: the antennal lobes, the fan shaped body, the lobula and a glomerulus of the posterior ventrolateral protocerebrum (summarized in Fig. 4.1A). Most of those areas mentioned, are part of *Drosophila* central complex (protocerebral bridge, fan shaped body, and noduli), which consists of interconnecting neuropils and act as an integration center receiving inputs from many parts of the brain for controlling visual and locomotion related behaviors (*Liu et al., 2006; Lin et al., 2013; Yang et al., 2013*). Furthermore, the evidence that we find FoxP to be expressed in both the optic lobes (medulla and lobula) (Fig. 3.1) and in motorneurons in the VNC (Fig. 3.3) strengthens the hypothesis that FoxP could be importantly involved in this pathway. Moreover, by looking at how the FoxP+ cell bodies localize in the brain (Fig. 4.1B), we recognized a prominent bilateral cell cluster known as DCN (*Hassan et al., 2000*) which consists of visual interneurons. It has been recently shown that this cluster is involved in object orientation and fixation (*Linneweber et al., 2020*), furthermore supporting the hypothesis of a role of FoxP in integrating visual stimuli (*Liu et al., 2006*) with locomotor

behavior. It is however to be taken in consideration that here we show that FoxP is widely expressed in other neuropils like the antennal lobes, that receive olfactory information (*Laissue et al., 1999; Ito et al., 2014*), the saddle, that corresponds to the antennal mechanosensory and motor center (*Chiang et al., 2011*), the gnathal ganglion, that refers to what used to be called subesophageal ganglion (*Chiang et al., 2011; Ito et al., 2014*) and the superior medial protocerebrum. Together with the finding that it is expressed in various cell types (Fig. 3.3), it is thus likely that FoxP may have a more complex function than how it was previously thought, and here we open the path for further studies on those areas.

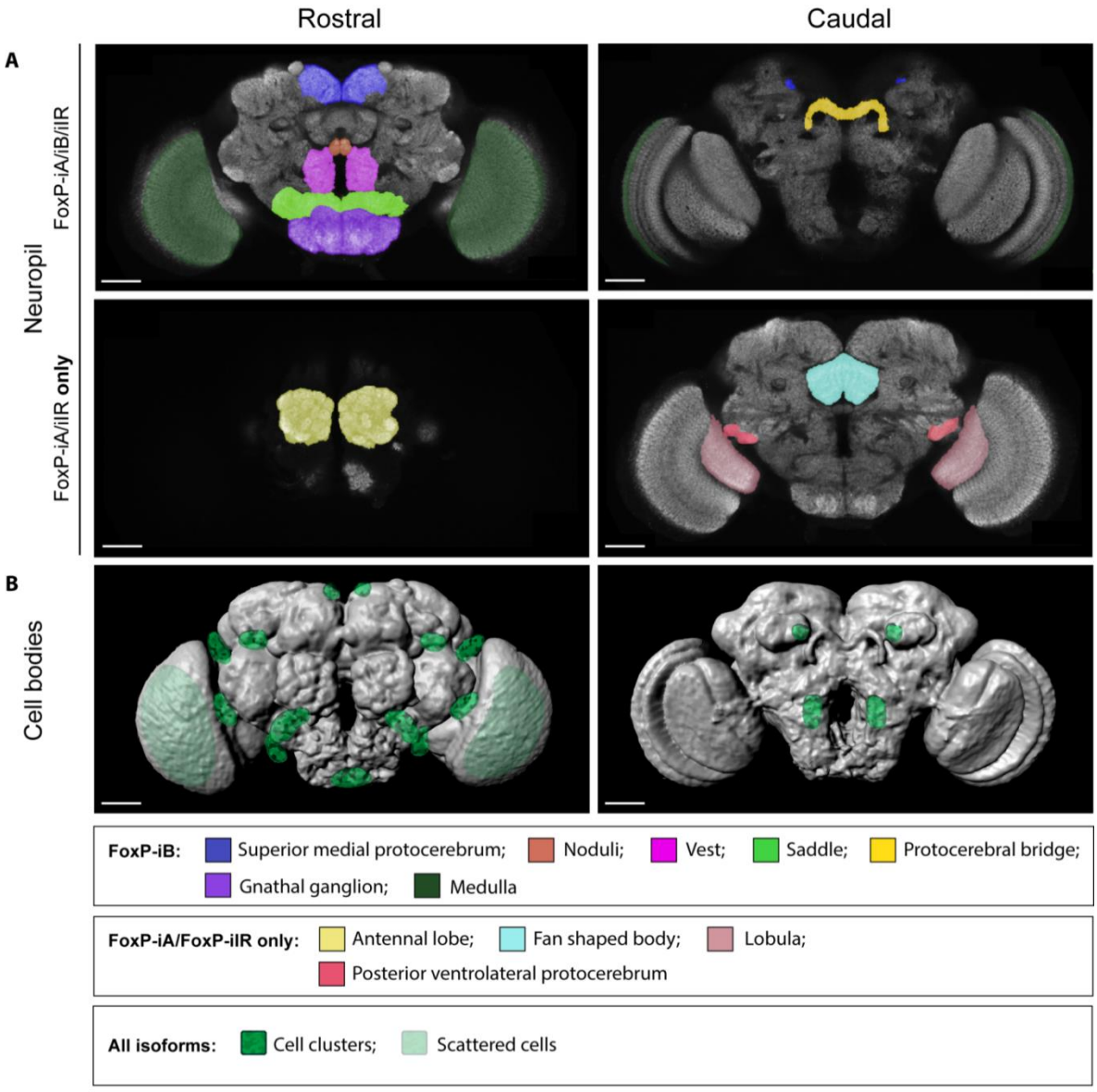

Fig. 4.1: *FoxP expression pattern in the adult Drosophila brain*. (A) Rostral and caudal sections with neuropil areas marked for *FoxP-iB* expression (above) or for other *FoxP* isoforms excluding *FoxP-iB* (below). (B) Volume rendering of adult neuropil with marked approximate *FoxP*-positive cell body locations in the cortex. Scale bars: 50 μm.

4.2 FoxP is required for normal locomotor behavior and object fixation

Once assessed the expression pattern of our lines, we were interested in seeing the resulting behavioral phenotype, in order to gain more detailed insight on FoxP function. All the behavioral experiments were performed with the Buridan's paradigm setup (*Colomb et al., 2012*), which gives detailed information on the locomotor behavior and object fixation of flies. We first performed the experiments on *FoxP-iB-Gal4* driver line (in this line the Gal4 sits and disrupts the DNA binding domain, preventing FoxP to act as a transcription factor) and *FoxP -/-* null mutant (Fig. 3.8, 9). What we see is a substantial loss of locomotor behavior and object fixation in the homozygous mutants if compared to the control for both lines, indicating that FoxP is essential for the flies in order to perform locomotion and fixate the two stripes; those data are supported by the locomotion experiment data from *Castells-Nobau et al., 2019*. Interestingly, we noticed that when it comes to heterozygous mutants, which have only one of the two alleles mutated, for some of the parameters considered the behavior seems to be enhanced if compared to controls. This phenomenon is called overdominance, which is a condition in genetics where the phenotype of the heterozygous lies outside the phenotypical range of both homozygous parents (*Hull, 1948; Parsons and Bodmer, 1961*). What we also noticed is that when we compare homozygous mutants from FoxP-iB and FoxP we do not see relevant differences between the two (Fig. 3.8F), indicating that isoform B absence is enough to trigger the phenotype. This may suggest that isoform B could have a more relevant role if compared to the other isoforms, which was already shown by *Mendoza et al., 2014* for another behavioral paradigm. What we did next was to exploit the conditional effector line we created, which was substantial for a better understanding the role of FoxP in the *Drosophila* nervous system. With this line it was possible to modulate FoxP KO in a spatio-temporal controlled manner, and this allowed us to understand FoxP's function in a more partitioned way. We saw that removing FoxP in motorneurons only or in the protocerebral bridge (Fig. 3.12) was already detrimental for the fly's locomotion and stripe fixation, thus supporting or previous

assumptions, while removing it in the DCN instead did not have any effect. Subsequently, we were interested in understanding if the role of FoxP in the *Drosophila* nervous system was or not developmental, and to answer this question we performed some temporal-specific KO at different stages of the fly's development. Interestingly, what we found is that the conditional KO of FoxP triggers a behavioral phenotype in the Buridan's paradigm only when performed during embryonal stage. No locomotor phenotype could be observed when the KO was performed in pupal or adult stage (Fig. 3.13), thus supporting the hypothesis of a developmental role for FoxP. However, it was recently shown by *Day et al., 2019* that FoxP2 in zebra finches plays an important role in maintenance of adult vocalizations, suggesting a novel role of this gene in longer term processes, which are yet to be analyzed in *Drosophila*.

To sum up, what we are proposing in this work are novel kind of mutants that allow to study FoxP expression (also considering the different isoforms) and behavior in a more detailed, versatile and specific way than how it was previously been done, paving the way for a comprehensive study on this thorny and contradictive transcription factor.

5. Conclusion

5.1 Conclusions and future perspectives

Here, we demonstrate that the *FoxP* gene is widely found in the *Drosophila* nervous system and that the different isoforms are differentially expressed in the numerous neuropil areas. Furthermore, we show that it is expressed in various neuronal types, suggesting that it may play a more complex role than previously thought. Even though, despite these advancements, it is still unknown in which processes and pathways FoxP is involved in the fly nervous system and, more precisely, which is the function of this transcription factor. In order to start elucidate this, it would be interesting to perform a DamID analysis to see FoxP target genes (*Aughey et al., 2019*). This technique permits a genome-wide profiling of DNA- or chromatin-binding proteins thanks to the fusion of the protein of interest with the Dam methylase, an enzyme that adds a methyl group to the adenine of the sequence 5'-GATC-3'. The resulting methylated DNA could then be sequenced to produce genome-wide binding profiles for the chromatin-interacting protein of interest that would thus ultimately allow to understand the downstream targets of FoxP and to have more detailed information on its function.

Here, we also show that FoxP is required for normal locomotor behavior and for fixation of motionless objects, and we have furthermore demonstrated that different neuropil areas/cell types or clusters are differentially involved in those kinds of behavior. In order to complete this information it would be worth to furthermore exploit our conditional effector line targeting the remaining neuropils (the more prominent being the fan shaped body and the antennal lobe) (Fig. 4.1A) and single cell type or cell clusters (Fig. 4.1B).

Another experiment that could be performed would be to create an additional conditional line, this time targeting FoxP-iB, in order to evaluate the role of this specific isoforms in the areas previously described.

Finally, as previously said, in this work we exclusively focused on locomotor behavior and stripe fixation, but being FoxP a pleiotropic gene, it was demonstrated (*Mendoza et al., 2014*) that it is also involved in other types of behavior, like operant self-learning. Thus, it would be important to understand which areas of the *Drosophila* nervous

system are involved in this kind of learning and to what extent, and this would be achieved by taking advantage again of our conditional FoxP effector line and testing it in the flight simulator set up (*Guo et al., 1996*) in various operant learning paradigms (*Brembs and Heisenberg, 2000; Brembs and Heisenberg, 2001; Brembs and Plendl, 2008*).

These last three experiments here listed are already about to be performed in our laboratory.

6. Bibliography

6.1 Research papers and reviews

Aughey, Gabriel N., Seth W. Cheetham, and Tony D. Southall. 2019. "DamID as a Versatile Tool for Understanding Gene Regulation." Development 146 (6). https://doi.org/10.1242/dev.173666.

Bacon, Claire, and Gudrun A. Rappold. 2012. "The Distinct and Overlapping Phenotypic Spectra of FOXP1 and FOXP2 in Cognitive Disorders." Human Genetics 131 (11): 1687–98. https://doi.org/10.1007/s00439-012-1193-z.

Bassett, Andrew, and Ji-Long Liu. 2014. "CRISPR/Cas9 Mediated Genome Engineering in Drosophila." Methods 69 (2): 128–36. https://doi.org/10.1016/j.ymeth.2014.02.019.

Becker, Martin, Paolo Devanna, Simon E. Fisher, and Sonja C. Vernes. 2018. "Mapping of Human FOXP2 Enhancers Reveals Complex Regulation." Frontiers in Molecular Neuroscience 11 (February): 47. https://doi.org/10.3389/fnmol.2018.00047.

Benjamin, D. J., Berger, J. O., Johannesson, M., Nosek, B. A., Wagenmakers, E.-J., Berk, R., Bollen, K. A., Brembs, B., Brown, L., Camerer. 2018. "Redefine statistical significance". Nature Human Behaviour, 2(1), 6–10.

Besson, Morgane, and Jean-René Martin. 2005. "Centrophobism/thigmotaxis, a New Role for the Mushroom Bodies in Drosophila." Journal of Neurobiology 62 (3): 386–96.

Brembs, B., and M. Heisenberg. 2000. "The Operant and the Classical in Conditioned Orientation of Drosophila Melanogaster at the Flight Simulator." Learning & Memory 7 (2): 104–15. https://doi.org/10.1101/lm.7.2.104.

———. 2001. "Conditioning with Compound Stimuli in Drosophila Melanogaster in the Flight Simulator." The Journal of Experimental Biology 204 (Pt 16): 2849–59. https://www.ncbi.nlm.nih.gov/pubmed/11683440.

Brembs, Björn, and Jan Wiener. 2006. "Context and Occasion Setting in Drosophila Visual Learning." Learning & Memory 13 (5): 618–28. https://doi.org/10.1101/lm.318606.

Brembs, Björn. 1996. "Classical and Operant Conditioning in Drosophila at the Flight Simulator." Julius-Maximilians-Universität Würzburg. https://epub.uni-regensburg.de/28513/1/brembs.pdf.

———. 2016. "Genetic Analysis of Behavior in Drosophila." e2491v1. PeerJ Preprints. https://doi.org/10.7287/peerj.preprints.2491v1

Castells-Nobau, Anna, Ilse Eidhof, Michaela Fenckova, Dova B. Brenman-Suttner, Jolanda M. Scheffer-de Gooyert, Sheren Christine, Rosa L. Schellevis, et al. 2019. “Conserved Regulation of Neurodevelopmental Processes and Behavior by FoxP in Drosophila.” PloS One 14 (2): e0211652. https://doi.org/10.1371/journal.pone.0211652.

Chabout, J., Sarkar, A., Patel, S. R., Radden, T., Dunson, D. B., Fisher, S. E., & Jarvis, E. D. 2016.” A Foxp2 Mutation Implicated in Human Speech Deficits Alters Sequencing of Ultrasonic Vocalizations in Adult Male Mice”. Frontiers in Behavioral Neuroscience, 10, 197.

Chiang, Ann-Shyn, Chih-Yung Lin, Chao-Chun Chuang, Hsiu-Ming Chang, Chang-Huain Hsieh, Chang-Wei Yeh, Chi-Tin Shih, et al. 2011. “Three-Dimensional Reconstruction of Brain-Wide Wiring Networks in Drosophila at Single-Cell Resolution.” Current Biology: CB 21 (1): 1–11. https://doi.org/10.1016/j.cub.2010.11.056.

Co, Marissa, Ashley G. Anderson, and Genevieve Konopka. 2020. “FOXP Transcription Factors in Vertebrate Brain Development, Function, and Disorders.” Wiley Interdisciplinary Reviews. Developmental Biology, January, e375. https://doi.org/10.1002/wdev.375.

Colomb, Julien, and Björn Brembs. 2016. “PKC in Motorneurons Underlies Self-Learning, a Form of Motor Learning in Drosophila.” PeerJ 4 (April): e1971. https://doi.org/10.7717/peerj.1971.

Colomb, Julien, Lutz Reiter, Jedrzej Blaszkiewicz, Jan Wessnitzer, and Bjoern Brembs. 2012. “Open Source Tracking and Analysis of Adult Drosophila Locomotion in Buridan’s Paradigm with and without Visual Targets.” PloS One 7 (8): e42247. https://doi.org/10.1371/journal.pone.0042247.

DasGupta, Shamik, Clara Howcroft Ferreira, and Gero Miesenböck. 2014. “FoxP Influences the Speed and Accuracy of a Perceptual Decision in Drosophila.” Science 344 (6186): 901–4. https://doi.org/10.1126/science.1252114.

Day, Nancy F., Taylor G. Hobbs, Jonathan B. Heston, and Stephanie A. White. 2019. “Beyond Critical Period Learning: Striatal FoxP2 Affects the Active Maintenance of Learned Vocalizations in Adulthood.” eNeuro 6 (2). https://doi.org/10.1523/ENEURO.0071-19.2019.

Diao, Fengqiu, Holly Ironfield, Haojiang Luan, Feici Diao, William C. Shropshire, John Ewer, Elizabeth Marr, Christopher J. Potter, Matthias Landgraf, and Benjamin H. White. 2015. “Plug-and-Play Genetic Access to Drosophila Cell Types Using Exchangeable Exon Cassettes.” Cell Reports 10 (8): 1410–21. https://doi.org/10.1016/j.celrep.2015.01.059.

Dolan, Michael-John, Ghislain Belliart-Guérin, Alexander Shakeel Bates, Shahar Frechter, Aurélie Lampin-Saint-Amaux, Yoshinori Aso, Ruairí J. V. Roberts, et al. 2018. “Communication from Learned to Innate Olfactory Processing Centers Is Required for Memory Retrieval in Drosophila.” Neuron 100 (3): 651–68.e8.

Doupe, A. J., and P. K. Kuhl. 1999. “Birdsong and Human Speech: Common Themes and Mechanisms.” Annual Review of Neuroscience 22: 567–631. https://doi.org/10.1146/annurev.neuro.22.1.567.

Duffy, Joseph B. 2002. “GAL4 System in Drosophila: A Fly Geneticist’s Swiss Army Knife.” Genesis 34 (1-2): 1–15. https://doi.org/10.1002/gene.10150.

Enard, Wolfgang. 2011. “FOXP2 and the Role of Cortico-Basal Ganglia Circuits in Speech and Language Evolution.” Current Opinion in Neurobiology 21 (3): 415–24. https://doi.org/10.1016/j.conb.2011.04.008.

Ernst, R., and M. Heisenberg. 1999. “The Memory Template in Drosophila Pattern Vision at the Flight Simulator.” Vision Research 39 (23): 3920–33. https://doi.org/10.1016/s0042-6989(99)00114-5.

Felsenberg, Johannes, Pedro F. Jacob, Thomas Walker, Oliver Barnstedt, Amelia J. Edmondson-Stait, Markus W. Pleijzier, Nils Otto, et al. 2018. “Integration of Parallel Opposing Memories Underlies Memory Extinction.” Cell 175 (3): 709–22.e15.

Fontenot, Jason D., Marc A. Gavin, and Alexander Y. Rudensky. 2003. “Foxp3 Programs the Development and Function of CD4+CD25+ Regulatory T Cells.” Nature Immunology 4 (4): 330–36. https://doi.org/10.1038/ni904.

French, C. A., Vinueza Veloz, M. F., Zhou, K., Peter, S., Fisher, S. E., Costa, R. M., & De Zeeuw, C. I. 2019. “Differential effects of Foxp2 disruption in distinct motor circuits”. Molecular Psychiatry, 24(3), 447–462.

Golson, Maria L., and Klaus H. Kaestner. 2016. “Fox Transcription Factors: From Development to Disease.” Development 143 (24): 4558–70. https://doi.org/10.1242/dev.112672.

Götz, K. G. 1980. “Visual Guidance in Drosophila.” Basic Life Sciences 16: 391–407. https://doi.org/10.1007/978-1-4684-7968-3_28.

Gratz, Scott J., C. Dustin Rubinstein, Melissa M. Harrison, Jill Wildonger, and Kate M. O’Connor-Giles. 2015. “CRISPR-Cas9 Genome Editing in Drosophila.” Current Protocols in Molecular Biology / Edited by Frederick M. Ausubel ... [et Al.] 111 (July): 31.2.1–31.2.20. https://doi.org/10.1002/0471142727.mb3102s111.

Gratz, Scott J., Fiona P. Ukken, C. Dustin Rubinstein, Gene Thiede, Laura K. Donohue, Alexander M. Cummings, and Kate M. O’Connor-Giles. 2014. “Highly Specific and Efficient CRISPR/Cas9-Catalyzed Homology-Directed Repair in Drosophila.” Genetics 196 (4): 961–71. https://doi.org/10.1534/genetics.113.160713.

Groschner, Lukas N., Laura Chan Wah Hak, Rafal Bogacz, Shamik DasGupta, and Gero Miesenböck. 2018. “Dendritic Integration of Sensory Evidence in Perceptual Decision-Making.” Cell 173 (4): 894–905.e13. https://doi.org/10.1016/j.cell.2018.03.075.

Guo, A., L. Li, S. Z. Xia, C. H. Feng, R. Wolf, and M. Heisenberg. 1996. “Conditioned Visual Flight Orientation in Drosophila: Dependence on Age, Practice, and Diet.” Learning & Memory 3 (1): 49–59. https://doi.org/10.1101/lm.3.1.49.

Haesler, Sebastian, Christelle Rochefort, Benjamin Georgi, Pawel Licznerski, Pavel Osten, and Constance Scharff. 2007. “Incomplete and Inaccurate Vocal Imitation after Knockdown of FoxP2 in Songbird Basal Ganglia Nucleus Area X.” PLoS Biology 5 (12): e321. https://doi.org/10.1371/journal.pbio.0050321.

Haesler, Sebastian, Kazuhiro Wada, A. Nshdejan, Edward E. Morrisey, Thierry Lints, Eric D. Jarvis, and Constance Scharff. 2004. “FoxP2 Expression in Avian Vocal Learners and Non-Learners.” The Journal of Neuroscience: The Official Journal of the Society for Neuroscience 24 (13): 3164–75. https://doi.org/10.1523/JNEUROSCI.4369-03.2004.

Hannenhalli, Sridhar, and Klaus H. Kaestner. 2009. “The Evolution of Fox Genes and Their Role in Development and Disease.” Nature Reviews. Genetics 10 (4): 233–40. https://doi.org/10.1038/nrg2523.

Hassan, B. A., N. A. Bermingham, Y. He, Y. Sun, Y. N. Jan, H. Y. Zoghbi, and H. J. Bellen. 2000. “Atonal Regulates Neurite Arborization but Does Not Act as a Proneural Gene in the Drosophila Brain.” Neuron 25 (3): 549–61. https://doi.org/10.1016/s0896-6273(00)81059-4.

Helfrich-Förster, Charlotte, Jörg Wulf, and J. Steven de Belle. 2002. “Mushroom Body Influence on Locomotor Activity and Circadian Rhythms in Drosophila Melanogaster.” Journal of Neurogenetics 16 (2): 73–109.

Heston, Jonathan B., and Stephanie A. White. 2015. “Behavior-Linked FoxP2 Regulation Enables Zebra Finch Vocal Learning.” The Journal of Neuroscience: The Official Journal of the Society for Neuroscience 35 (7): 2885–94. https://doi.org/10.1523/JNEUROSCI.3715-14.2015.

Heyer, Wolf-Dietrich, Kirk T. Ehmsen, and Jie Liu. 2010. “Regulation of Homologous Recombination in Eukaryotes.” Annual Review of Genetics 44: 113–39. https://doi.org/10.1146/annurev-genet-051710-150955.

Hoed, Joery den, and Simon E. Fisher. 2020. “Genetic Pathways Involved in Human Speech Disorders.” Current Opinion in Genetics & Development 65 (July): 103–11. https://doi.org/10.1016/j.gde.2020.05.012.

Horn, Carsten, and Alfred M. Handler. 2005. “Site-Specific Genomic Targeting in Drosophila.” Proceedings of the National Academy of Sciences of the United States of America 102 (35): 12483–88. https://doi.org/10.1073/pnas.0504305102.

Horn, Denise, Johannes Kapeller, Núria Rivera-Brugués, Ute Moog, Bettina Lorenz-Depiereux, Sebastian Eck, Maja Hempel, et al. 2010. “Identification of FOXP1 Deletions in Three Unrelated Patients with Mental Retardation and Significant Speech and Language Deficits.” Human Mutation 31 (11): E1851–60. https://doi.org/10.1002/humu.21362.

Horvath, Philippe, and Rodolphe Barrangou. 2010. “CRISPR/Cas, the Immune System of Bacteria and Archaea.” Science 327 (5962): 167–70. https://doi.org/10.1126/science.1179555.

Hull, F. H. 1948. “Evidences of Overdominance in Yield of Corn.” Genetics 33 (1): 110. https://www.ncbi.nlm.nih.gov/pubmed/18903861.

Iliakis, G., H. Wang, A. R. Perrault, W. Boecker, B. Rosidi, F. Windhofer, W. Wu, J. Guan, G. Terzoudi, and G. Pantelias. 2004. “Mechanisms of DNA Double Strand Break Repair and Chromosome Aberration Formation.” Cytogenetic and Genome Research 104 (1-4): 14–20. https://doi.org/10.1159/000077461.

Ito, Kei, Kazunori Shinomiya, Masayoshi Ito, J. Douglas Armstrong, George Boyan, Volker Hartenstein, Steffen Harzsch, et al. 2014. “A Systematic Nomenclature for the Insect Brain.” Neuron 81 (4): 755–65. https://doi.org/10.1016/j.neuron.2013.12.017.

Jackson, Brian C., Christopher Carpenter, Daniel W. Nebert, and Vasilis Vasiliou. 2010. “Update of Human and Mouse Forkhead Box (FOX) Gene Families.” Human Genomics 4 (5): 345–52. https://doi.org/10.1186/1479-7364-4-5-345.

Jinek, Martin, Krzysztof Chylinski, Ines Fonfara, Michael Hauer, Jennifer A. Doudna, and Emmanuelle Charpentier. 2012. “A Programmable Dual-RNA-Guided DNA Endonuclease in Adaptive Bacterial Immunity.” Science 337 (6096): 816–21. https://doi.org/10.1126/science.1225829

Jinek, Martin, Krzysztof Chylinski, Ines Fonfara, Michael Hauer, Jennifer A. Doudna, and Emmanuelle Charpentier. 2012. “A Programmable Dual-RNA-Guided DNA Endonuclease in Adaptive Bacterial Immunity.” Science 337 (6096): 816–21. https://doi.org/10.1126/science.1225829.

Kiya, T., Y. Itoh, and T. Kubo. 2008. “Expression Analysis of the FoxP Homologue in the Brain of the Honeybee, Apis Mellifera.” Insect Molecular Biology 17 (1): 53–60. https://doi.org/10.1111/j.1365-2583.2008.00775.x.

Kondo, Shu, and Ryu Ueda. 2013. “Highly Improved Gene Targeting by Germline-Specific Cas9 Expression in Drosophila.” Genetics 195 (3): 715–21. https://doi.org/10.1534/genetics.113.156737.

König, Christian, Afshin Khalili, Thomas Niewalda, Shiqiang Gao, and Bertram Gerber. 2019. “An Optogenetic Analogue of Second-Order Reinforcement in Drosophila.” Biology Letters 15 (7): 20190084.

Kosubek-Langer, Jennifer, and Constance Scharff. 2020. “Dynamic FoxP2 Levels in Male Zebra Finches Are Linked to Morphology of Adult-Born Area X Medium Spiny Neurons.” Scientific Reports 10 (1): 4787. https://doi.org/10.1038/s41598-020-61740-6.

Laissue, P. P., C. Reiter, P. R. Hiesinger, S. Halter, K. F. Fischbach, and R. F. Stocker. 1999. “Three-Dimensional Reconstruction of the Antennal Lobe in Drosophila Melanogaster.” The Journal of Comparative Neurology 405 (4): 543–52. https://www.ncbi.nlm.nih.gov/pubmed/10098944.

Lark, Arianna, Toshihiro Kitamoto, and Jean-René Martin. 2017. “Modulation of Neuronal Activity in the Drosophila Mushroom Body by DopEcR, a Unique Dual Receptor for Ecdysone and Dopamine.” Biochimica et Biophysica Acta, Molecular Cell Research 1864 (10): 1578–88.

Lawton, Kristy J., Taryn L. Wassmer, and David L. Deitcher. 2014. “Conserved Role of Drosophila Melanogaster FoxP in Motor Coordination and Courtship Song.” Behavioural Brain Research 268 (July): 213–21. https://doi.org/10.1016/j.bbr.2014.04.009.

Lawton, Kristy. 2014. “Conserved Role Of Drosophila Melanogaster Foxp In Motor Coordination And Courtship Song.” Edited by David Lawrence Deitcher. PhD, Cornell University. https://ecommons.cornell.edu/handle/1813/36103.

Lebreton, Sébastien, and Jean-René Martin. 2009. “Mutations Affecting the cAMP Transduction Pathway Disrupt the Centrophobism Behavior.” Journal of Neurogenetics 23 (1-2): 225–34.

Lieber, Michael R. 2010. “The Mechanism of Double-Strand DNA Break Repair by the Nonhomologous DNA End-Joining Pathway.” Annual Review of Biochemistry 79: 181–211. https://doi.org/10.1146/annurev.biochem.052308.093131.

Lin, Chih-Yung, Chao-Chun Chuang, Tzu-En Hua, Chun-Chao Chen, Barry J. Dickson, Ralph J. Greenspan, and Ann-Shyn Chiang. 2013. “A Comprehensive Wiring Diagram of the Protocerebral Bridge for Visual Information Processing in the Drosophila Brain.” Cell Reports 3 (5): 1739–53. https://doi.org/10.1016/j.celrep.2013.04.022.

Linneweber, Gerit Arne, Maheva Andriatsilavo, Suchetana Bias Dutta, Mercedes Bengochea, Liz Hellbruegge, Guangda Liu, Radoslaw K. Ejsmont, et al. 2020. “A Neurodevelopmental Origin of Behavioral Individuality in the Drosophila Visual System.” Science 367 (6482): 1112–19. https://doi.org/10.1126/science.aaw7182.

Liu, Gang, Holger Seiler, Ai Wen, Troy Zars, Kei Ito, Reinhard Wolf, Martin Heisenberg, and Li Liu. 2006. “Distinct Memory Traces for Two Visual Features in the Drosophila Brain.” Nature 439 (7076): 551–56. https://doi.org/10.1038/nature04381.

Lu, Min Min, Shanru Li, Honghua Yang, and Edward E. Morrisey. 2002. “Foxp4: A Novel Member of the Foxp Subfamily of Winged-Helix Genes Co-Expressed with Foxp1 and Foxp2 in Pulmonary and Gut Tissues.” Mechanisms of Development 119 Suppl 1 (December): S197–202. https://doi.org/10.1016/s0925-4773(03)00116-3.

Lyutova, Radostina, Mareike Selcho, Maximilian Pfeuffer, Dennis Segebarth, Jens Habenstein, Astrid Rohwedder, Felix Frantzmann, Christian Wegener, Andreas S. Thum, and Dennis Pauls. 2019. “Reward Signaling in a Recurrent Circuit of Dopaminergic Neurons and Peptidergic Kenyon Cells.” Nature Communications 10 (1): 3097.

Mabuchi, Ikumi, Naoto Shimada, Shoma Sato, Kahori Ienaga, Show Inami, and Takaomi Sakai. 2016. “Mushroom Body Signaling Is Required for Locomotor Activity Rhythms in Drosophila.” Neuroscience Research 111 (October): 25–33.

Manjila, Steffy B., Maria Kuruvilla, Jean-Francois Ferveur, Sanjay P. Sane, and Gaiti Hasan. 2019. “Extended Flight Bouts Require Disinhibition from GABAergic Mushroom Body Neurons.” Current Biology: CB 29 (2): 283–93.e5.

Martin, J. R., R. Ernst, and M. Heisenberg. 1998. “Mushroom Bodies Suppress Locomotor Activity in Drosophila Melanogaster.” Learning & Memory 5 (1-2): 179–91.

McGuire, Sean E., Phuong T. Le, Alexander J. Osborn, Kunihiro Matsumoto, and Ronald L. Davis. 2003. “Spatiotemporal Rescue of Memory Dysfunction in Drosophila.” Science 302 (5651): 1765–68. https://doi.org/10.1126/science.1089035.

McGuire, Sean E., Zhengmei Mao, and Ronald L. Davis. 2004. “Spatiotemporal Gene Expression Targeting with the TARGET and Gene-Switch Systems in Drosophila.” Science’s STKE: Signal Transduction Knowledge Environment 2004 (220): l6. https://doi.org/10.1126/stke.2202004pl6.

Meerschaut, Ilse, Daniel Rochefort, Nicole Revençu, Justine Pètre, Christina Corsello, Guy A. Rouleau, Fadi F. Hamdan, et al. 2017. “FOXP1-Related Intellectual Disability Syndrome: A Recognisable Entity.” Journal of Medical Genetics 54 (9): 613–23. https://doi.org/10.1136/jmedgenet-2017-104579.

Mendoza, Ezequiel, Julien Colomb, Jürgen Rybak, Hans-Joachim Pflüger, Troy Zars, Constance Scharff, and Björn Brembs. 2014. “Drosophila FoxP Mutants Are Deficient in Operant Self-Learning.” PloS One 9 (6): e100648. https://doi.org/10.1371/journal.pone.0100648.

Palumbo, O., D'Agruma, L., Minenna, A. F., Palumbo, P., Stallone, R., Palladino, T., Zelante, L., & Carella, M. (2013). 3p14.1 de novo microdeletion involving the FOXP1 gene in an adult patient with autism, severe speech delay and deficit of motor coordination. Gene, 516(1), 107–113.

Parsons, P. A., and W. F. Bodmer. 1961. "The Evolution of Overdominance: Natural Selection and Heterozygote Advantage." Nature 190 (April): 7–12. https://doi.org/10.1038/190007a0.

Pollock, J. A., M. H. Ellisman, and S. Benzer. 1990. "Subcellular Localization of Transcripts in Drosophila Photoreceptor Neurons: Chaoptic Mutants Have an Aberrant Distribution." Genes & Development 4 (5): 806–21. https://doi.org/10.1101/gad.4.5.806.

Port, Fillip, and Simon L. Bullock. 2016. "Augmenting CRISPR Applications in Drosophila with tRNA-Flanked sgRNAs." Nature Methods 13 (10): 852–54. https://doi.org/10.1038/nmeth.3972.

Reuter, M. S., Riess, A., Moog, U., Briggs, T. A., Chandler, K. E., Rauch, A., Stampfer, M., Steindl, K., Gläser, D., Joset, P., DDD Study, Krumbiegel, M., Rabe, H., et al.. (2017). FOXP2 variants in 14 individuals with developmental speech and language disorders broaden the mutational and clinical spectrum. Journal of Medical Genetics, 54(1), 64–72.

Roote, John, and Andreas Prokop. 2013. "How to Design a Genetic Mating Scheme: A Basic Training Package for Drosophila Genetics." G3 3 (2): 353–58. https://doi.org/10.1534/g3.112.004820.

Rueden, Curtis T., Johannes Schindelin, Mark C. Hiner, Barry E. DeZonia, Alison E. Walter, Ellen T. Arena, and Kevin W. Eliceiri. 2017. "ImageJ2: ImageJ for the next Generation of Scientific Image Data." BMC Bioinformatics 18 (1): 529. https://doi.org/10.1186/s12859-017-1934-z.

Santos, M. Emília, Alekos Athanasiadis, Alexandre B. Leitão, Louis DuPasquier, and Elio Sucena. 2011. "Alternative Splicing and Gene Duplication in the Evolution of the FoxP Gene Subfamily." Molecular Biology and Evolution 28 (1): 237–47. https://doi.org/10.1093/molbev/msq182.

Schatton, Adriana, and Constance Scharff. 2016. "Next Stop: Language. The 'FOXP2' Gene's Journey through Time." Mètode Science Studies Journal - Annual Review 0 (7). https://doi.org/10.7203/metode.7.7248.

Serway, Christine N., Rebecca R. Kaufman, Roland Strauss, and J. Steven de Belle. 2009. "Mushroom Bodies Enhance Initial Motor Activity in Drosophila." Journal of Neurogenetics 23 (1-2): 173–84.

Shan, Qiwei, Yanpeng Wang, Jun Li, Yi Zhang, Kunling Chen, Zhen Liang, Kang Zhang, et al. 2013. "Targeted Genome Modification of Crop Plants Using a CRISPR-Cas System." Nature Biotechnology 31 (8): 686–88. https://doi.org/10.1038/nbt.2650.

Shimeld, Sebastian M., Bernard Degnan, and Graham N. Luke. 2010. “Evolutionary Genomics of the Fox Genes: Origin of Gene Families and the Ancestry of Gene Clusters.” Genomics 95 (5): 256–60. https://doi.org/10.1016/j.ygeno.2009.08.002.

Shu, Weiguo, Min Min Lu, Yuzhen Zhang, Philip W. Tucker, Deying Zhou, and Edward E. Morrisey. 2007. “Foxp2 and Foxp1 Cooperatively Regulate Lung and Esophagus Development.” Development 134 (10): 1991–2000. https://doi.org/10.1242/dev.02846.

Siper, Paige M., Silvia De Rubeis, Maria Del Pilar Trelles, Allison Durkin, Daniele Di Marino, François Muratet, Yitzchak Frank, et al. 2017. “Prospective Investigation of FOXP1 Syndrome.” Molecular Autism 8 (October): 57. https://doi.org/10.1186/s13229-017-0172-6.

Skinner, B. F. 1938. “The Behavior of Organisms: An Experimental Analysis” 457. https://psycnet.apa.org/fulltext/1939-00056-000.pdf.

———. 1963. “Operant Behavior.” The American Psychologist 18 (8): 503–15. https://doi.org/10.1037/h0045185

Sokolowski, M. B. 2001. “Drosophila: Genetics Meets Behaviour.” Nature Reviews. Genetics 2 (11): 879–90. https://doi.org/10.1038/35098592.

Song, Xiaomin, Bin Li, Yan Xiao, Chunxia Chen, Qiang Wang, Yujie Liu, Alan Berezov, et al. 2012. “Structural and Biological Features of FOXP3 Dimerization Relevant to Regulatory T Cell Function.” Cell Reports 1 (6): 665–75. https://doi.org/10.1016/j.celrep.2012.04.012.

Sun, Jun, An Qi Xu, Julia Giraud, Haiko Poppinga, Thomas Riemensperger, André Fiala, and Serge Birman. 2018. “Neural Control of Startle-Induced Locomotion by the Mushroom Bodies and Associated Neurons in.” Frontiers in Systems Neuroscience 12 (March): 6.

Takahashi, Hiroshi, Kaoru Takahashi, and Fu-Chin Liu. 2009. “FOXP Genes, Neural Development, Speech and Language Disorders.” Advances in Experimental Medicine and Biology 665: 117–29. https://doi.org/10.1007/978-1-4419-1599-3_9.

Thum, Andreas S., and Bertram Gerber. 2019. “Connectomics and Function of a Memory Network: The Mushroom Body of Larval Drosophila.” Current Opinion in Neurobiology 54 (February): 146–54.

Turrel, Oriane, Valérie Goguel, and Thomas Preat. 2018. “Amnesiac Is Required in the Adult Mushroom Body for Memory Formation.” The Journal of Neuroscience: The Official Journal of the Society for Neuroscience 38 (43): 9202–14.

Wang, Bin, Joel Weidenfeld, Min Min Lu, Shanna Maika, William A. Kuziel, Edward E. Morrisey, and Philip W. Tucker. 2004. “Foxp1 Regulates Cardiac Outflow Tract, Endocardial Cushion Morphogenesis

and Myocyte Proliferation and Maturation." Development 131 (18): 4477–87. https://doi.org/10.1242/dev.01287.

Warth Pérez Arias, Carmina Carelia, Patrizia Frosch, André Fiala, and Thomas D. Riemensperger. 2020. "Stochastic and Arbitrarily Generated Input Patterns to the Mushroom Bodies Can Serve as Conditioned Stimuli in." Frontiers in Physiology 11 (February): 53.

Weigel, D., G. Jürgens, F. Küttner, E. Seifert, and H. Jäckle. 1989. "The Homeotic Gene Fork Head Encodes a Nuclear Protein and Is Expressed in the Terminal Regions of the Drosophila Embryo." Cell 57 (4): 645–58. https://doi.org/10.1016/0092-8674(89)90133-5.

Widmer, Yves F., Cornelia Fritsch, Magali M. Jungo, Silvia Almeida, Boris Egger, and Simon G. Sprecher. 2018. "Multiple Neurons Encode CrebB Dependent Appetitive Long-Term Memory in the Mushroom Body Circuit." eLife 7 (October). https://doi.org/10.7554/eLife.39196.

Xie, Kabin, Bastian Minkenberg, and Yinong Yang. 2015. "Boosting CRISPR/Cas9 Multiplex Editing Capability with the Endogenous tRNA-Processing System." Proceedings of the National Academy of Sciences of the United States of America 112 (11): 3570–75. https://doi.org/10.1073/pnas.1420294112.

Xiong, Yan, Hailong Lv, Zhefeng Gong, and Li Liu. 2010. "Fixation and Locomotor Activity Are Impaired by Inducing Tetanus Toxin Expression in Adult Drosophila Brain." Fly 4 (3): 194–203.

Yang, Jacob S., Takeshi Awasaki, Hung-Hsiang Yu, Yisheng He, Peng Ding, Jui-Chun Kao, and Tzumin Lee. 2013. "Diverse Neuronal Lineages Make Stereotyped Contributions to the Drosophila Locomotor Control Center, the Central Complex." The Journal of Comparative Neurology 521 (12): 2645–Spc1. https://doi.org/10.1002/cne.23339.

6.2 Websites

https://bdsc.indiana.edu/

https://blast.ncbi.nlm.nih.gov/Blast.cgi

https://flybase.org

https://web.expasy.org/translate/

https://www.ncbi.nlm.nih.gov/Structure/cdd/wrpsb.cgi

https://www.virtualflybrain.org

7. Attachments

7.1 Supplementary figures

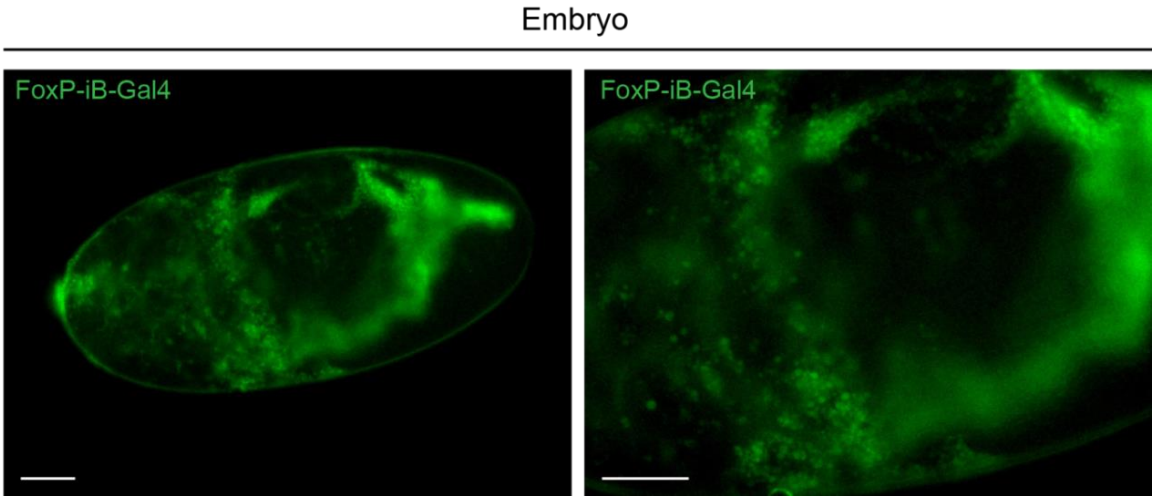

Fig. S1: *FoxP-iB is expressed in the early embryo*. The non-confocal image of an embryo from the cross of our *FoxP-iB-Gal4* driver line with a *UAS-Stinger-GFP* shows that FoxP-iB is expressed very early during embryonal development. Scale bars: 50 μm.

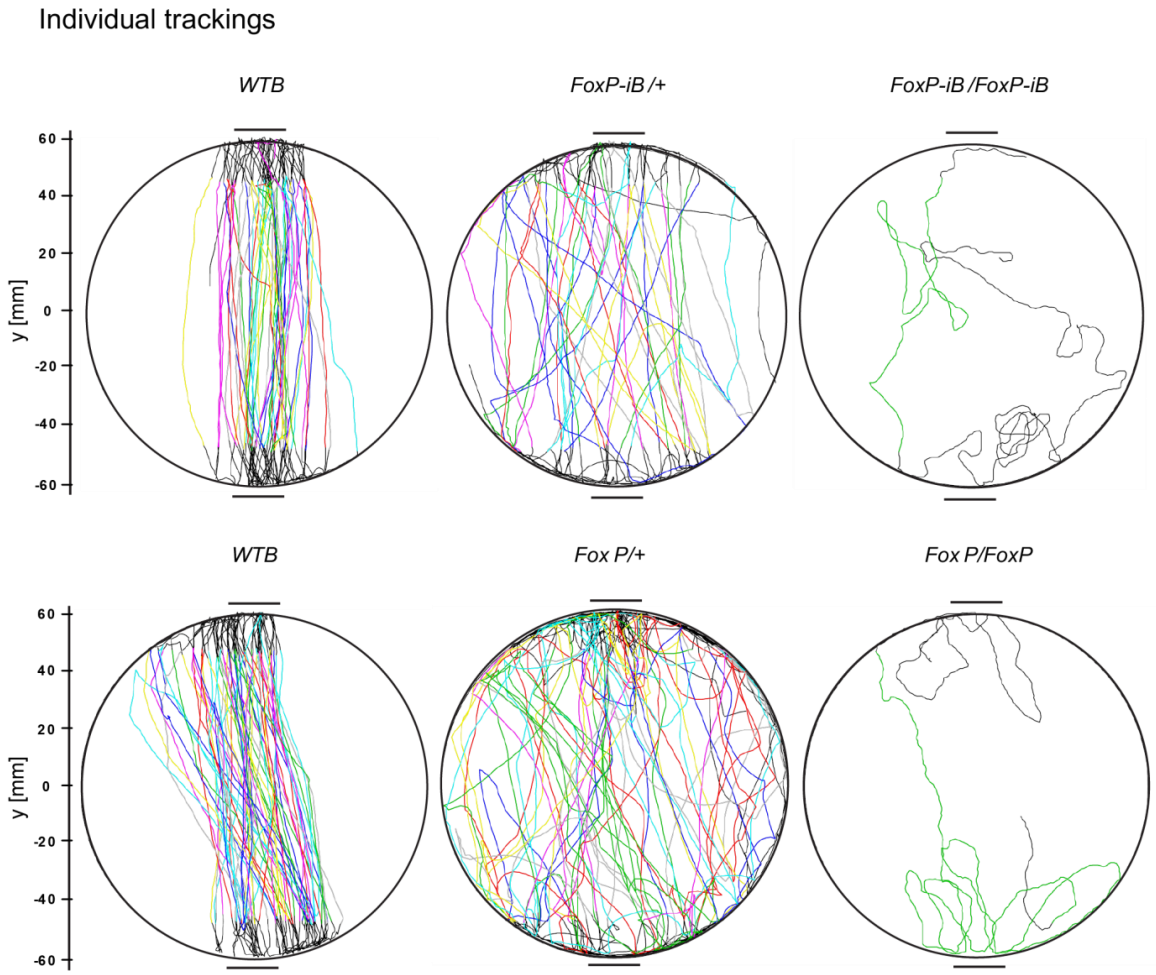

Fig. S2: *Single trajectories of the flies in the Buridan's paradigm*. Example of some trajectories that the single flies perform in the Buridan's paradigm set up show that *WTB* flies execute a straighter path between the stripes if compared to heterozygous mutant and homozygous mutant for both FoxP-iB (upper row) and FoxP (lower row).

8. List of figures

9. List of tables

10. Acknowledgements

Hoping to do justice to everybody,

First and foremost I would like to thank my supervisor Prof. Dr. Björn Brembs for giving me the chance of doing here my PhD, for believing in me and for being always present in times of need. Thank you for making this an interesting, fun and rewarding adventure.

Secondly I surely want to thank Dr. Mathias Raß, without whom I probably would not have done half of what I did. Thank you for teaching me, being patient (sometimes 😜), being a good listener and a good friend.

Thank you to Prof. Dr. Stefan Schneuwly, for mentoring, for providing insightful comments to this project and for the generosity of letting me use a lot of your lab equipment. Thank you Stefan and also many thanks to Juan, Laura, Svenja, Jose, Ushi, Suzanne, Renate and Christa for the friendly lab environment.

I then would like to thank Matthias Schramm for the nice and fun chats about our love problems, the pauses with you were always full of laughs and tears (the latter mostly mine 😊), thank you also for the help you gave me in the lab when I was stressed (so almost always 😁).

I want now to thank my sweet Marcela. Thank you for being almost like a mum here, thank you for your kind words and for your never ending support. Thank you for teaching me Spanish and thank you for always lifting my spirit up ❤. Muchas gracias.

Thank you to Andi, for being a polite colleague and for teaching me how to be strong and resilient. Thank you to Christian for being now a precious friend and before the best office mate anybody could ask for, the room is still empty without you in it 💔.

I also would like to thank Prof. Dr. Diana Pauly for always being nice and sweet, and for the help and support provided at the Klinikum. Thank you also for being an example of brave woman. Thank you then to my friend Nicole, you are one of the nicest people I know! Thank you for the time spent chatting, eating and drinking together, and for

being always so wise ☺. You are going to be a great scientist. A special thanks goes also to Yassin, for the nice and fun lunches spent at Unikat and for the looooooong monologues that I always loved to listen ☺ (sayonara 😁).

Then, a big thank you also to the *RIGeL* queens: Kinga and Caroline! Thank you for skillfully solving every problem, thank you for your hard work and kind heart 😘

Now I would like to thank all of the people that were with me every step of the way outside work and that made this journey in Germany fun and bright:

A huge thank you goes to the *Italian gang*: Giulia (the Archeologist), Marta, Martino, Luigi, and Roberto (the Mathematicians), Elia (the Politician), Antonio (the Physicist), Raffaella (the Architect), Claudia (the Biochemist), Anna and Nicolò (the Inorganic chemists). You made my days (and especially my evenings/nights) unforgettable! The Oktoberfest, the numerous Dult and Palmator, the Spanish parties, the Christmas parties, the dinners, the nights at Beats and so much more! We created amazing memories together. Thanks to you all also for sharing the joys and the pains of being PhDs students. Grazie di cuore!

I want now to thank some non-Italian friends (yes, I was able to make some of them too 😁): thank you to Selina, you have won a special place in my heart ♥, you are the sweetest know-it-all I have ever met and Christian is lucky to have you! Thank you for exchanging gossips, knowledge and most of all, teachings 😁. Thank you to my sweetie-pie Mathilde, to Lina, Luisa and to Felix, you made me love ants almost more than flies (…Björn if you are reading this, I am joking! 😁), thank you for the support provided in summer schools (and R courses) and for the fun outside the university. Thank you also to Drew for the amazing conversations about snow, Christmas, and Norway.

Thank you to my friends in Italy that supported me in the choice of going abroad: thank you to my oldest friend Cecilia, for being there since forever, thank you to Erica for the laughters and thank you to Claudio for having loved me, no matter how it ended.

I now want to say thank you my parents (Marco and Fabrizia) for always believing in me and being present, supportive, helpful, caring and loving. I am lucky to have you as

my parents. Thank you to my little sister Donata, you can be a real pain the ~~ass~~ but I love you more than anything and I will always be there for you when you need me. Thank you to Federico, for taking care of my sister and for being part of the family.

Last but definitely not least I want to say thank you to my significant *otter* César. Thank you for being the perfect boyfriend, for being sweet, smart and for teaching me how to be patient and how to be a better person. Thank you for showing me how to see past my own nose. Thank you for just being there always. Te quiero tanto ♥.

Bonus section: relevant movies to watch

Gattaca

The Fly

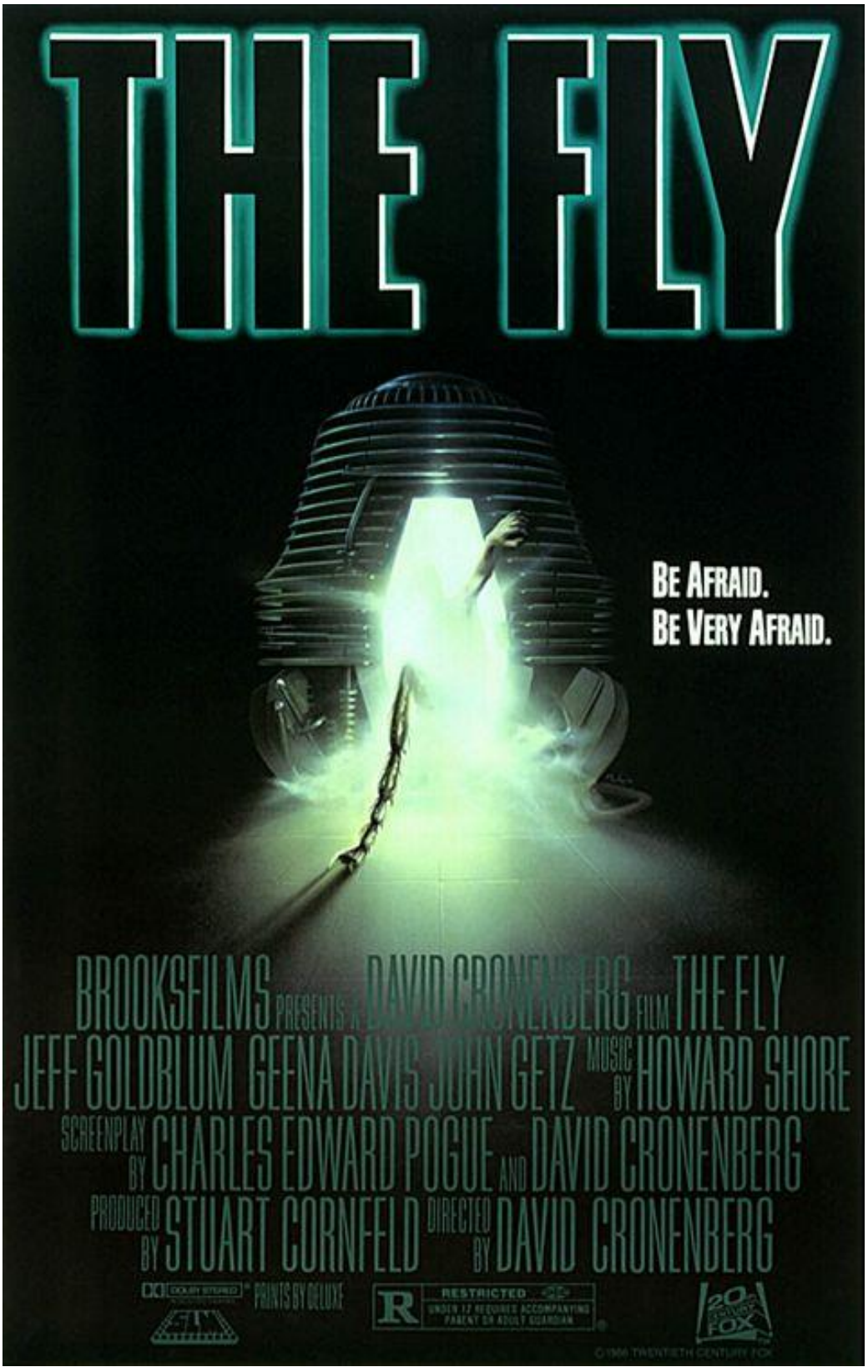
THE FLY
BE AFRAID.
BE VERY AFRAID.
BROOKSFILMS PRESENTS A DAVID CRONENBERG FILM THE FLY
JEFF GOLDBLUM GEENA DAVIS JOHN GETZ MUSIC BY HOWARD SHORE
SCREENPLAY BY CHARLES EDWARD POGUE AND DAVID CRONENBERG
PRODUCED BY STUART CORNFELD DIRECTED BY DAVID CRONENBERG
DOLBY STEREO
PRINTS BY DELUXE
R
RESTRICTED
UNDER 17 REQUIRED ACCOMPANYING PARENT OR ADULT GUARDIAN
20th CENTURY FOX

Eidesstattliche Erklärung

(1) Ich erkläre hiermit an Eides statt, dass ich die vorliegende Arbeit ohne unzulässige Hilfe Dritter und ohne Benutzung anderer als der angegebenen Hilfsmittel angefertigt habe; die aus anderen Quellen direkt oder indirekt übernommenen Daten und Konzepte sind unter Angabe des Literaturzitats gekennzeichnet.

(2) Bei der Auswahl und Auswertung folgenden Materials haben mir die nachstehend aufgeführten Personen in der jeweils beschriebenen Weise entgeltlich/unentgeltlich geholfen:

1. .....

2. .....

3. .....

(3) Weitere Personen waren an der inhaltlich-materiellen Herstellung der vorliegenden Arbeit nicht beteiligt. Insbesondere habe ich hierfür nicht die entgeltliche Hilfe eines Promotionsberaters oder anderer Personen in Anspruch genommen. Niemand hat von mir weder unmittelbar noch mittelbar geldwerte Leistungen für Arbeiten erhalten, die im Zusammenhang mit dem Inhalt der vorgelegten Dissertation stehen.

(4) Die Arbeit wurde bisher weder im In- noch im Ausland in gleicher oder ähnlicher Form einer anderen Prüfungsbehörde vorgelegt.

Regensburg, den

Ottavia Palazzo